

Geochemistry and petrogenesis of the Miocene alkaline and sub-alkaline volcanic rocks from the Chagai arc, Baluchistan, Pakistan: Implications for porphyry Cu-Mo-Au deposits

Rehanul Haq Siddiqui¹, M. Asif Khan² and M. Qasim Jan³

¹ Geoscience Laboratory, Geological Survey of Pakistan, Shahzad Town, Islamabad

² National Centre of Excellence in Geology, University of Peshawar, Pakistan

³ Quaid-i-Azam University, Islamabad, Pakistan

Abstract

The Miocene volcanic rocks are developed in the western part of an EW trending subduction related magmatic belt known as the Chagai arc in the Baluchistan province of Pakistan. The volcanism in this arc initiated during the Late Cretaceous, which intermittently continued up to the Quaternary period. In the regional geotectonic context this arc belongs to the Tethyan convergence zone and is believed to have formed due to the northward subduction of Arabian oceanic plate beneath the southern margin of Afghan micro plate and hence is considered as an Andean-type arc.

The Miocene volcanic and volcanoclastic rocks form a gently dipping caldera of a collapse stratovolcano. This volcanic caldera is intruded by several tonalite porphyry stocks, hosting porphyry copper deposits. These volcanics are described as Buze Mashi Koh Volcanic Group and are mainly represented by interstratified andesitic lava flows and volcanoclastics including agglomerates, tuffs, lapilli tuffs and volcanic breccia. Towards the northern side of the volcanic caldera, basaltic lava flows are also found.

The petrological studies reveal that Miocene volcanic rocks comprise mainly basaltic-andesite, andesite, basaltic-trachyandesite and trachyandesite. Two distinct series, sub-alkaline (0.73-1.66 wt. % K₂O) and alkaline (2.94-4.69 wt. % K₂O) are recognized based on petrochemical studies. The sub-alkaline basaltic rocks have high magnesium MgO (8.12-11.38 wt. %) Mg # (68-69), Co (28-42 ppm), Ni (286-307 ppm) and Cr (662-720 ppm) suggestive of their direct derivation from the partial melting of a sub-arc mantle source. The alkaline rocks have lower Mg # (44-59) and lower contents of Mg, Co, Ni and Cr. Their primordial mantle-normalized trace element patterns show enrichment in all the incompatible trace elements, marked negative Nb anomalies and generally positive spikes on Ba and Sr, which strongly confirm their island arc signatures. The chondrite-normalized REE patterns show high and variable enrichment of LREE and negative Eu anomalies, suggesting fractionation of plagioclase during differentiation. Plots in various tectonomagmatic discrimination diagrams depict that these rocks were erupted in a continental-margin type arc environment. Enrichment of most incompatible trace element and greatly enhanced Zr/Y (9.67), Ti/V (31.83), Ti/Zr (34.67), Ba/Y (53.29), Th/Y (0.39) La/Yb_N (23.44), Ta/Yb (0.58), Th/Yb (6.01) ratios relative to N-MORB indicate that parent magma of both the volcanic series was derived from an enriched sub-arc mantle source. The Zr versus Zr/Y and Cr versus Y plots suggest that parent magma of these rock suites was generated by the partial melting of about 15-25 % enriched sub-arc mantle source. A comparison of the Oligocene-Miocene volcanic rocks with other analogous rocks of the Chagai arc show relatively enhanced values of LILE and LREE. This suggests that during the Miocene, which is also the time of emplacement of several porphyry copper deposits in the Chagai arc, fluids enriched in LILE and LREE emanating from the subducting slab of oceanic crust were added to the sub-arc mantle source in greater abundances. This high rate of addition of these fluids is postulated to be related with the rapid and shallow subduction of Arabian oceanic plate below the Zagros-Makran convergence zone that might be related with the opening and rapid spreading of the Red Sea during this period. This suggests that during the Oligocene period which is the time of emplacement of several porphyry copper deposits in the Chagai arc; comparatively more LILE and LREE enriched fluids from the subducting slab of oceanic crust were added to the sub-arc mantle source.

1. Introduction

The Chagai arc, which occurs in the Balochistan province, of Pakistan is one of the metallogenically most important mountain belts in Pakistan as many economic

metal deposits including porphyry (Mo-Au-Ag), manto and vein type copper, stratiform and skarn type iron, volcanogenic gold-silver and sulphur, kuroko type lead-zinc-silver-copper are found intimately associated with its magmatic rocks (Siddiqui, 1996; Perello et al., 2008). The

Miocene volcanic and volcanoclastic rocks are developed in the western part of the arc and occur at about 65 km SE of Amalaf (Fig. 1) as a collapse volcanic caldera. This volcanic caldera is intruded by several tonalite porphyry stocks, hosting porphyry copper deposits. These volcanic rocks are described as Buze Mashi Koh Volcanic Group and are mainly represented by interstratified andesitic lava flows and volcanoclastic rocks including agglomerates, tuffs, lapilli tuffs and volcanic breccia. Towards the northern side of the volcanic caldera, basaltic lava flows are also found.

The present study is the first systematic account of the field relations, petrography and geochemistry of the Miocene volcanic rocks of the Chagai arc. One of the principal findings of the study includes realization that whereas the Late Cretaceous to Paleocene volcanic rocks did form in oceanic island arc setting, the Eocene volcanic rocks represented a transitional character between oceanic and continental island arcs. And the younger volcanic rocks (i.e., Oligocene to Quaternary) have composition suggestive of their origin in continental margin type setting.

In this paper we present a detailed study of the Miocene volcanic rocks of the Chagai arc in terms of their petrogenesis and to demonstrate their origin as continental margin type setting. Finally an attempt has been made to explore possible genetic relationship between these and other Neogene volcanic rocks and the porphyry copper deposits in the region.

2. Geological setting

The major part of the Chagai arc is situated in the western part of the Baluchistan province of Pakistan; a small part of it also extends towards west in Iran and towards north in Afghanistan. Overall the Chagai arc occupies an area of 75,000 km² with an EW general trend. (Fig. 1). The arc is convex towards south (Spector and Associates Ltd., 1981; Farah et al., 1984) and is terminated by the Chaman transform fault zone in the east and Harirud fault zone in the west.

The Pioneer geological work in the Chagai-Raskoh arc terrane was carried out by Vredenburg as early as 1901. Hunting Survey Corporation (1960) conducted reconnaissance study and geological mapping of the entire Balochistan province on 1:253,440. During the seventies, many foreign geologists, including Sillitoe (1978), Nigell (1975), Dykstra (1978), Arthurton et al. (1979) and Britzman (1979) studied the Chagai arc. They considered the Chagai arc as an Andean-type calc-alkaline magmatic belt, constructed on the southern leading edge of the Afghan microplate, but no petrological or geochemical data were presented in support of this hypothesis. Ahmed (1984) also upheld a similar view on the basis of major elements chemistry of some acidic intrusive rocks. Siddiqui et al.

(1986; 1987; 1988) and Siddiqui (1996) performed initial petrological studies, recorded tholeiitic, calc-alkaline and alkaline magmatism and proposed oceanic island arc affinities for the Late Cretaceous to Paleocene volcanics, transitional character for the Eocene volcanics and continental margin type arc settings for the younger (i.e. Oligocene to Quaternary) volcanics. Regional geological mapping of the Chagai island arc on 1:50,000 scale, which was initiated by the Geological Survey of Pakistan in 1960, is still in progress.

The oldest rock unit of the Chagai arc is the Cretaceous Sinjrani Volcanic Group. The Group was intruded during Late Cretaceous to Pleistocene by Chagai plutons of various compositions including granite, adamellite, granodiorite, tonalite, diorite and gabbro. Other rock units exposed in the Chagai arc are Humai Formation (Late Cretaceous), Juzzak/Rakshani Formation (Paleocene), Saindak Formation (Eocene), Robat Limestone (Early to Middle Eocene), Amalaf Formation (Oligocene), Dalbandin Formation (Miocene to Pleistocene), Buze Mashi Koh Volcanic Group (Miocene), Koh-e-Sultan Volcanic Group (Pliocene to Pleistocene) and semi to unconsolidated subrecent and recent deposits. The Miocene volcanic and volcanoclastic rocks occur in western part of the Chagai arc (Fig. 1). The stratigraphic sequence in the Chagai arc is presented in Fig. 2.

The Miocene volcanics are situated at about 65 km SE of Amalaf (Fig. 1). They consist of volcanic and volcanoclastic rocks, forming a gently dipping (5°-15°) caldera of a collapse stratovolcano (Fig. 3 and 4). This caldera is intruded by several tonalite porphyry stocks hosting porphyry copper deposits. These volcanic rocks described as Buze Mashi Koh Volcanic Group (Siddiqui, 2004), mainly consist of interstratified andesitic lava flows and volcanoclastics, including agglomerates, tuffs, lapilli tuffs and volcanic breccia. Towards the northern side of the caldera basaltic lava flows are also encountered (Fig. 4B). The various volcanic and volcanoclastic rocks of Buze Mashi Koh Volcanic Group are described below:

Agglomerates: The agglomerates are pale to dark green in colour and occur as 1.5 to 6 m thick strata. They are composed of subrounded, 5 cm - 1 m size fragments of porphyritic andesite and tuff embedded in a hard and compact volcanic ash matrix.

Tuffs: The tuffs are mostly green to brownish green in colour and form 1 to 3 m thick beds. They are composed of 1 - 3 cm size fragments of andesitic rocks embedded in a fine and compact ash matrix. The lapilli tuffs exhibit the same colour and thickness of strata as tuffs. They are composed of subangular to subrounded, 3 mm - 1.5 cm size fragments of porphyritic andesite and tuffs embedded in a fine-grained tuffaceous matrix.

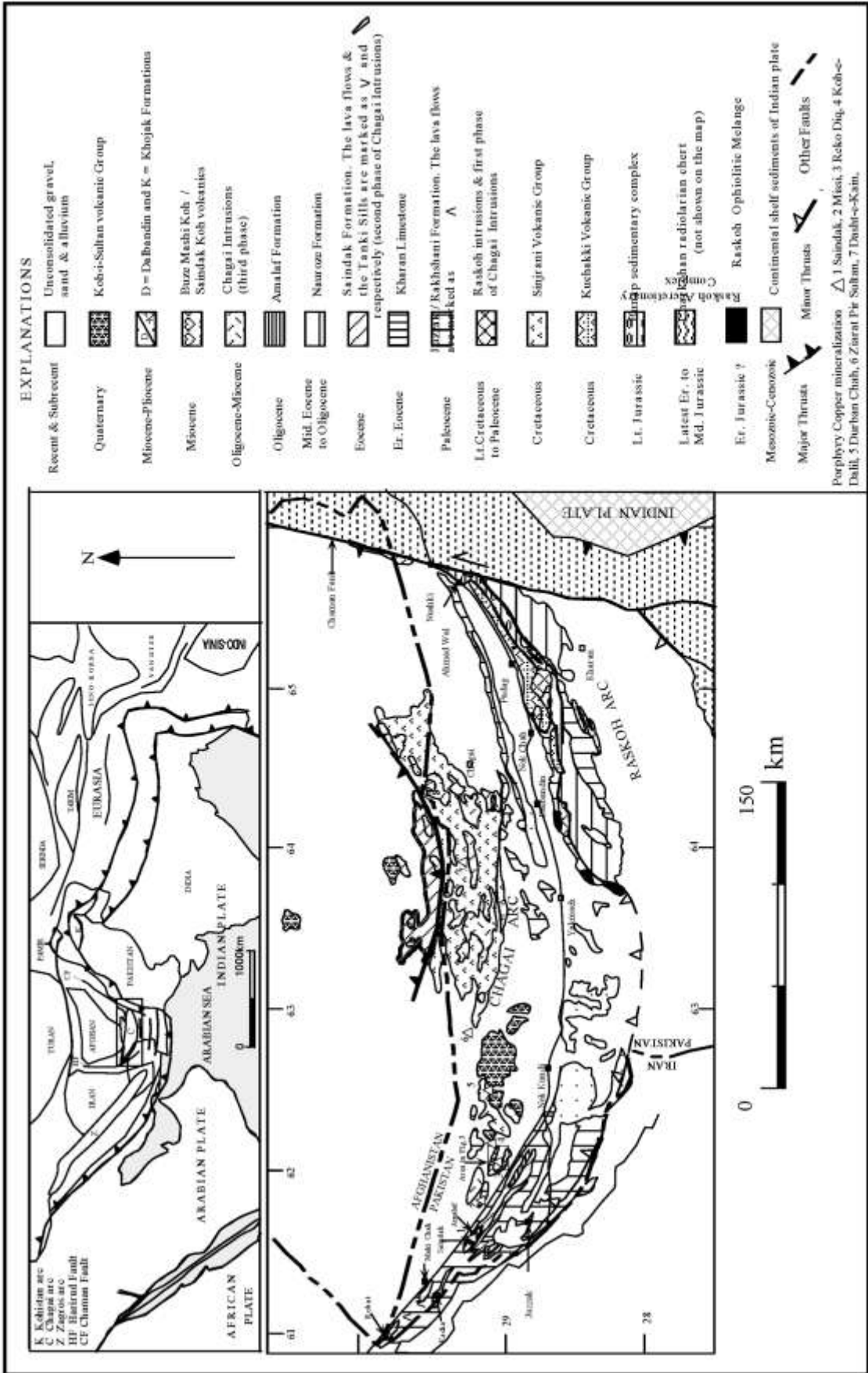


Fig. 1. Geological map of the chagai-Raskoh arc terrane, Balochistan, Pakistan (modified and reproduced after Bakr and Jackson, 1964; Siddiqui, 2004).

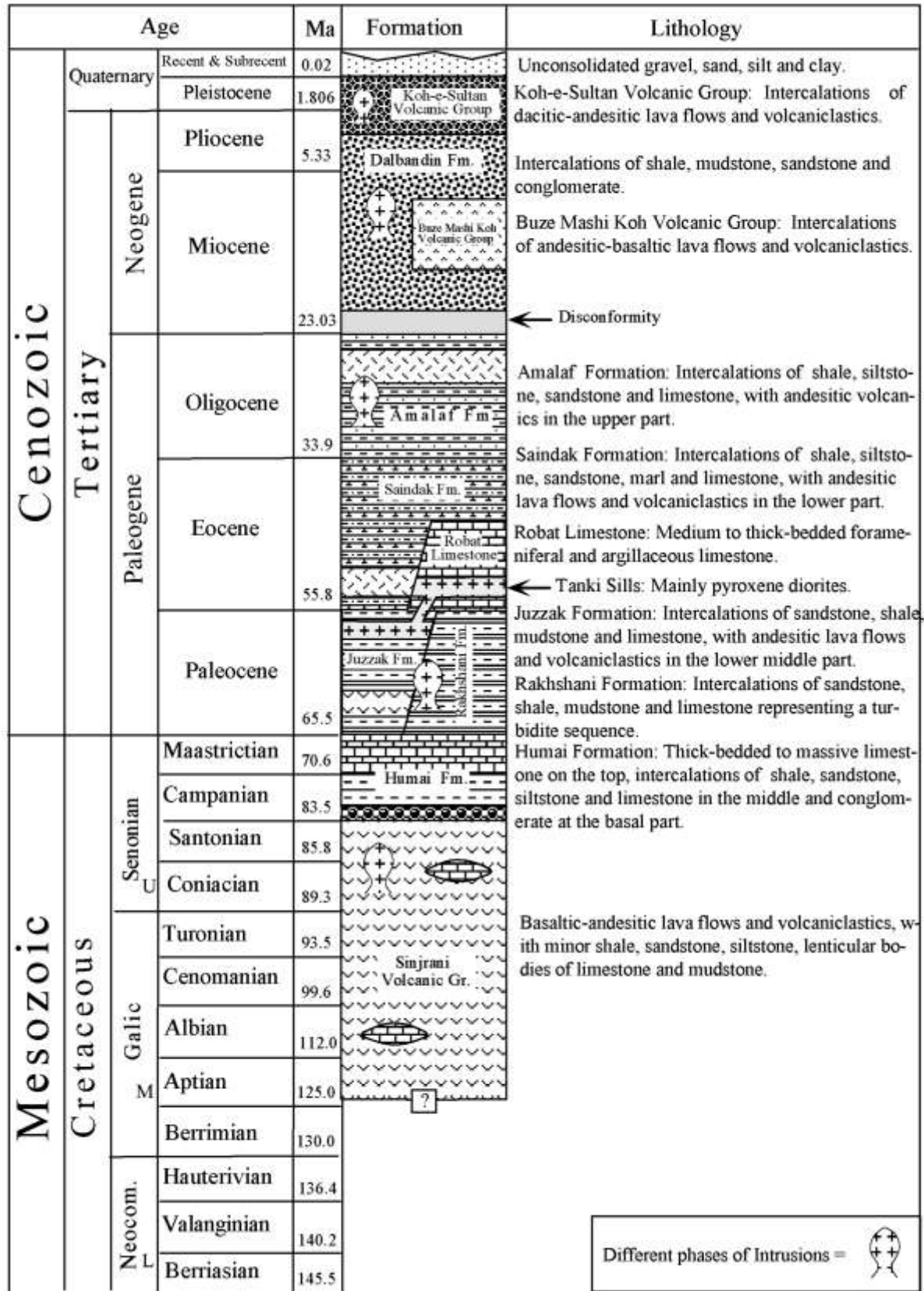


Fig. 2. Generalized stratigraphic sequence in the Chagai arc (based on Jones, 1960; Siddiqui, 2004). The time scale is after Ogg et al. (2008).

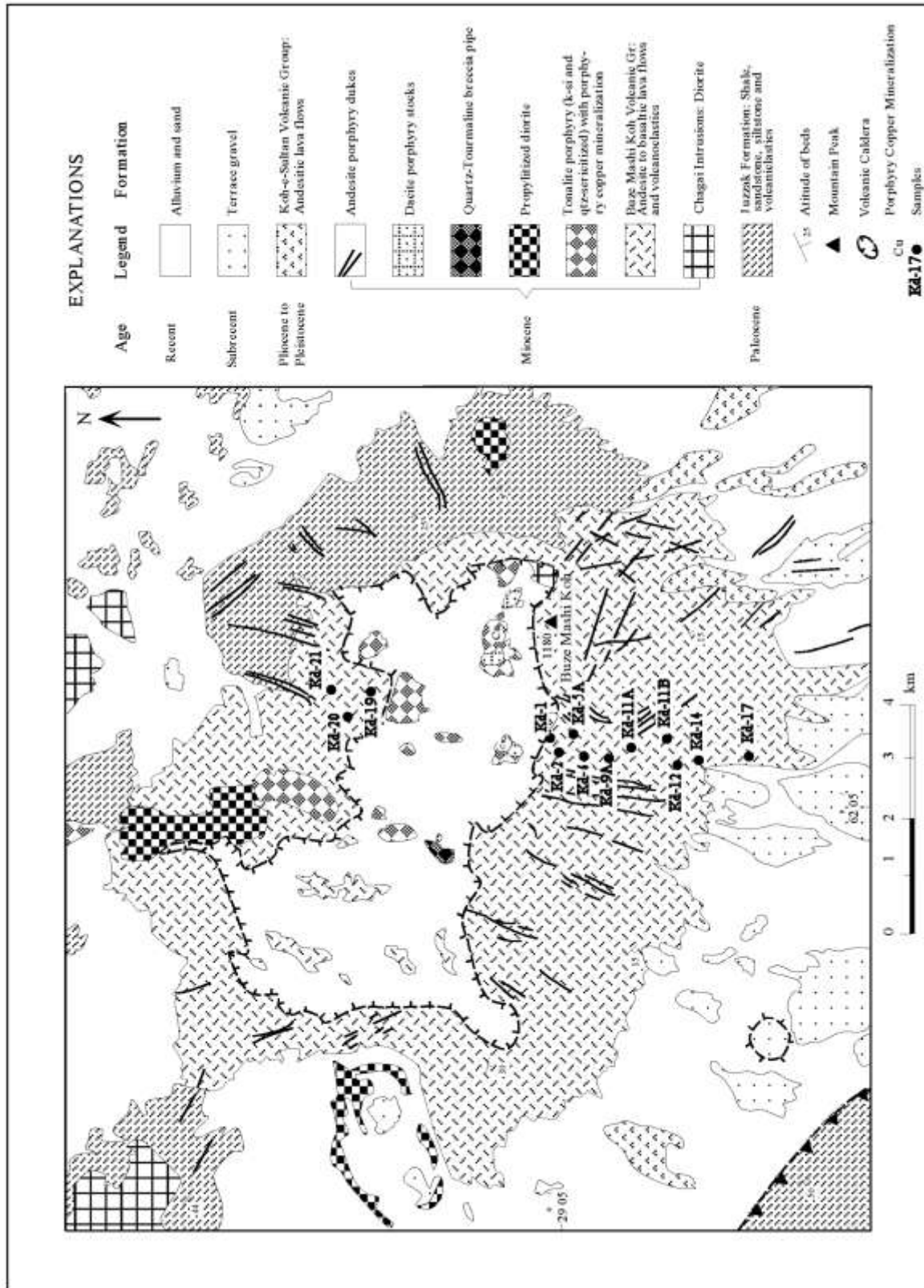


Fig. 3. Geological map of Buze Mashi Koh area (modified and reproduced after Khan and Ahmad, 1981; Siddiqui, 2004).

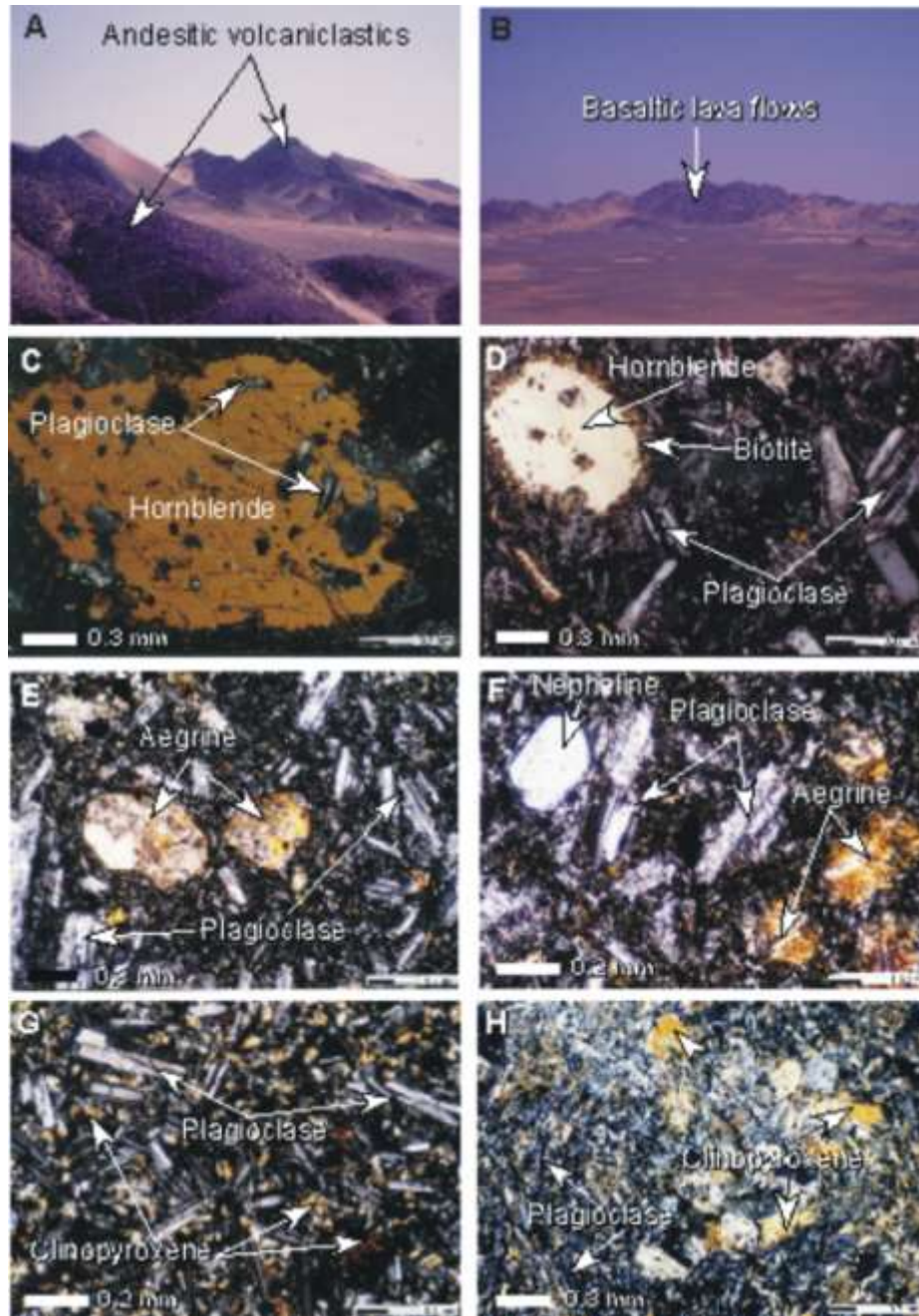


Fig. 4. (A) Western part of the Buze Mashi Koh volcanic caldera in the west-central part of the Chagai arc. View looking towards north, (B) Basaltic lava flows on the northern flank of Buze Mashi Koh volcanic caldera in the west-central part of the Chagai arc. View looking towards north, (C) Photomicrograph of an andesite (Kd-1) displaying large phenocrysts of hornblende with small inclusions of plagioclase. Note the rounded outline and reaction rim of biotite around the hornblende phenocryst, (D) Another photomicrograph of andesite (Kd-1) displaying a phenocrysts of hornblende (with reaction rim of biotite.) and plagioclase in a groundmass comprising tinny crystals of plagioclase, hornblende, opaques and volcanic glass, (E) Photomicrograph of a porphyritic trachyandesite (Kd-2) exhibiting phenocrysts of aegirine (centre) and plagioclase embedded in a micro-cryptocrystalline groundmass having the same minerals, (F) Photomicrograph displaying intersertal texture formed in basalt (Kd-19) by the occurrences of small prismatic crystals and anhedral grains of clinopyroxene in interstices between the larger crystals of plagioclase. (G) Photomicrograph exhibiting cumulo-phyric and pilotaxitic textures formed in basalt (Kd-19) by parallel orientation of plagioclase crystals around clustered olivine phenocrysts, (H) Photomicrograph displaying cumulo-phyric texture formed in basalt (Kd-21) by clustering of clinopyroxene phenocryst. Note also the trachytic texture displayed by plagioclase. All photomicrograph are in crossed polarized light.

Lava flows: The lava flows are greyish green to dark green in colour and form 1 to 3 m thick beds. They are andesitic in composition and are fine-grained and porphyritic in texture. These are highly weathered and partially chloritized. Phenocrysts of pyroxene, hornblende and plagioclase can be seen with naked eyes. Basaltic lava flows occur in a restricted area in the northern flanks of the stratovolcano. They form about 300 m thick sequence of inseparable volcanic eruptions, which extend up to 500 m. These are dark, compact and form relatively higher and rugged physiography. The basalt is dark green to black in colour and microporphyritic in texture. K-Ar dating gives a 12.8 ± 0.3 Ma age to these volcanics (Siddiqui, 1996).

3. Petrography

3.1. Andesites/Trachyandesites

These rocks are hypocrySTALLINE, porphyritic and intersertal in texture and amygdaloidal in nature (Fig. 4C and D). Phenocrysts of plagioclase and amphibole (nepheline and aegirine in case of trachyandesite) are embedded in a micro to cryptocrystalline and devitrified groundmass, having tiny laths (<1 mm), microlites, and crystallites of plagioclase and amphibole. Phenocrysts to groundmass ratio ranges from 35 : 65 to 40 : 60.

Plagioclase: The plagioclase crystals are euhedral to subhedral, lath-like and tabular in shape and exhibit polysynthetic twinning according to the albite and occasionally to the combined albite and Carlsbad laws. Oscillatory zoning is also developed in some of the plagioclase crystals. The plagioclase phenocrysts are andesine, ranging in composition from An₃₈ to An₄₂. The groundmass plagioclase generally occurs as small microlites, crystallites, and tiny columnar laths. Small columnar crystals of plagioclase are also found as inclusions in the larger crystals of hornblende.

Feldspathoids: The feldspathoids are mainly represented by nepheline, which only occurs in trachyandesite. It occurs as small untwined euhedral phenocrysts showing parallel extinction.

Pyroxene: The pyroxene is represented by aegirine (Fig. 4F) in the trachyandesites, and occurs as small euhedral to subhedral prismatic crystals with eight sided basal sections. It shows light green to green pleochroism and occasionally shows twinning.

Amphibole: The amphibole is mainly represented by hornblende, which occurs as large euhedral to subhedral prismatic crystals with six sided basal sections showing well-developed cleavages. It shows yellow to green pleochroism and occasionally shows twinning. At

places large phenocrysts of hornblende exhibit reaction rims of biotite. The groundmass hornblende occurs as small euhedral and prismatic crystals and globules in interstices between the small plagioclase crystals imparting to the rock an intersertal texture.

Accessory Minerals: Apatite, magnetite, titanomagnetite and hematite are common accessories. Apatite occurs as small euhedral and prismatic crystals enclosed in larger crystals of plagioclase. Magnetite occurs as small subhedral to anhedral crystals scattered throughout the groundmass and also found as inclusions in hornblende phenocrysts. Hematite occurs as partial to complete replacement of magnetite crystals.

Secondary Minerals: Secondary minerals are generally developed as partial or complete replacement of primary minerals, or infillings in vesicles. Biotite and chlorite are the common alteration products of hornblende. The larger crystals of hornblende are partially replaced by biotite. Clay minerals, sericite, and calcite have developed as a result of partial alteration of plagioclase.

Amygdules: Rocks are moderately vesiculated. Vesicles are generally filled with chlorite, calcite, zeolite and volcanic glass. In some vesicles, chlorite occurs in the centre and zeolites form linings towards the margin.

3.2. Basalts/Trachybasalts

Under microscope these rocks are hypocrySTALLINE, microporphyritic, intersertal, subcumulophyric and trachytic in texture (Fig. 4G and H). Small phenocrysts of pyroxene, olivine and plagioclase are embedded in a microcrystalline groundmass of the same minerals. The phenocrysts to groundmass ratio is generally 30 : 70.

Plagioclase: The plagioclase crystals are euhedral to subhedral, lath-like and tabular in shape and exhibit polysynthetic twinning according to the albite and occasionally to the combined albite and Carlsbad laws. The anorthite contents of plagioclase generally ranges from 38 to 53, which falls within the andesine-labradorite range. The groundmass, plagioclase occurs as small microlites, crystallites, and tiny columnar laths. The plagioclase microlites show some alignment imparting a trachytic texture to the rock.

Orthoclase: Substantial amount of orthoclase is also found in the groundmass of alkali basalts, and occurs as small euhedral crystals and exhibits Carlsbad twinning.

Olivine: Olivine occurs as small anhedral phenocrysts, partially to completely serpentinized. In some samples small anhedral phenocrysts occur in clusters forming a cumulophyric texture (Fig. 5G).

Pyroxene: The Pyroxene is mainly represented by diopside augite, which occurs as large euhedral to subhedral prismatic crystals partially to completely replaced by uralite. It occasionally shows twinning. The groundmass pyroxene is also uralitized and found as small prismatic and anhedral crystals. At places small prismatic crystals of uralite make clusters forming a cumulo-phyric texture (Fig. 4H).

Accessory Minerals: Apatite, sphene and titanomagnetite occur as accessory minerals. Very small acicular crystals of apatite occur in larger crystals of plagioclase. Titanomagnetite occurs as small subhedral to anhedral crystals scattered throughout the groundmass. Small thin-rhomboidal crystals of sphene are also scattered throughout the groundmass.

Secondary Minerals: Secondary minerals are generally developed as partial or complete replacement of primary minerals, or infillings in vesicles. Uralite and chlorite are the common alteration products of pyroxene. Sericite and calcite have developed due to partial alteration of plagioclase. Hematite occurs as partial to complete replacement of titanomagnetite crystals.

Amygdules: Rocks are moderately vesiculated. Vesicles are generally filled with chlorite. The rock ranges in composition from alkali basalt to sub-alkali basalt.

4. Geochemistry

Thirteen rock samples were collected from the Miocene volcanic rocks of the Chagai arc. All the samples were analyzed for major and trace elements. Five of the samples were also analyzed for rare earth elements (REE). Bulk chemical analyses of samples from these volcanic rocks are given in Table 1. The major elements are recalculated on a volatile free basis, because some of the samples show loss on ignition up to 4.18 wt. % due to alteration.

4.1. Analytical techniques

4.1.1. Major and trace elements analyses

The major and trace elements were analyzed in the Geoscience Laboratory, Geological Survey of Pakistan, Islamabad, by X-ray fluorescence spectrometry (RIGAKU XRF-3370E). The sample powder (<200 mesh), weighing 0.7g was thoroughly mixed with 3.5g of lithium tetra borate (flux). The analyses were carried out on 1 : 5 rock powder and flux fused disks commonly known as glass beads. The samples thus obtained were analyzed by XRF using corresponding GSJ (Geological Survey of Japan) standard samples

with every batch of ten samples. The results of analyses were then compared with the recommended values of USGS (United State Geological Survey) standard reference samples. A check of precision of the instrument was made using JA-3 standard sample (Govindaraju, 1989).

4.1.2. Rare earth elements analyses

The analysis of rare earth elements (REE) and Hf, Th, U and Ta was carried out in the GSJ using ICP-MS 2000 (YOKOGAWA, Japan). About 200 g of powdered sample (<200 mesh) was weighed in a platinum dish and 3ml HClO₄, 4ml HNO₃ and 5ml HF was added to the sample. The sample was then heated on the hot plate at 200°C till complete evaporation. The dish was removed from the hot plate, cooled, washed and dried. The residue was added 5ml 1 : 1 HNO₃ and 5ml water and gently heated on the hot plate till complete dissolution. The solution in the dish was cooled and filtered. The filtrate was transferred into a 100ml measuring flask and added water up to 100ml mark. The solution thus obtained was analyzed by ICP-MS, following Imai (1990) method, using JB-1 and JA-1 as standard samples (Govindaraju, 1989) and 1.5% HNO₃ as blank sample. The detection limits of ICP-MS 2000 for all these elements are <0.1 ppm. A check of precision of the instrument was made using JB-1 and JA-1 standard samples (Govindaraju, 1989).

4.2. Classification

All the rock samples are plotted in SiO₂ versus alkali (wt%) diagrams (Fig. 5) of Le Bas et al. (1986). In this diagram four samples plot in basalt field, one in basaltic-andesite, one in andesite, four in basaltic-trachyandesite and three in trachyandesite fields. The superimposition of a dashed line demarcating the alkaline and sub-alkaline (Irvine and Baragar, 1971) shows that Miocene volcanics plotting in basaltic trachyandesite and trachyandesite (together with one sample plotting in basalt field) are alkaline, while the rest are sub-alkaline. Since alkali elements (Na₂O and K₂O) are susceptible to mobilization in response to alteration / metasomatism / metamorphism, a classification scheme based on high-field strength elements is used for verification. In this context, all the samples from Miocene volcanic rocks are plotted in Zr/TiO₂ versus Nb/Y diagrams (Winchester and Floyd, 1977). In this diagram two samples plot in sub-alkaline basalt, one in basaltic andesite, one in andesite, four in alkali basalt and four in trachyandesite fields (Fig. 6). In the light of classification scheme based on these two diagrams and values in Table 1 different sample legends are used for alkaline, sub-alkaline rocks in all the figures.

Table 1. Bulk chemistry of Miocene volcanic rocks from the Chagai arc.

| | Sub-alkaline | | | | | Alkaline | |
|------------------------------------|--------------|--------|-------|-------|-------|----------|--------|
| | Kd-19 | Kd-20 | Kd-21 | Kd-17 | Kd-1 | Kd-5A | Kd-9A |
| SiO ₂ | 48.69 | 48.17 | 47.69 | 56.71 | 59.32 | 46.52 | 50.7 |
| TiO ₂ | 1.15 | 1.13 | 1.12 | 0.79 | 0.58 | 1.44 | 1.88 |
| Al ₂ O ₃ | 15.53 | 15.42 | 15.2 | 19.06 | 18.2 | 17.06 | 19.12 |
| Fe ₂ O ₃ | 9.71 | 10.05 | 10.44 | 7.08 | 6.35 | 11.43 | 8.86 |
| MnO | 0.2 | 0.19 | 0.18 | 0.12 | 0.15 | 0.3 | 0.16 |
| MgO | 10.29 | 10.99 | 11.38 | 3.18 | 3.56 | 8.12 | 4.00 |
| CaO | 11.39 | 10.7 | 10.29 | 7.96 | 7.11 | 9.84 | 8.46 |
| Na ₂ O | 1.9 | 1.73 | 1.66 | 3.92 | 3.57 | 1.7 | 2.16 |
| K ₂ O | 0.73 | 1.29 | 1.66 | 0.97 | 0.93 | 2.94 | 4.69 |
| P ₂ O ₅ | 0.4 | 0.39 | 0.38 | 0.2 | 0.23 | 0.65 | 0.66 |
| FeOt/MgO | 0.84 | 0.81 | 0.82 | 1.98 | 1.59 | 1.25 | 1.97 |
| Na ₂ O/K ₂ O | 2.6 | 1.34 | 1 | 4.04 | 3.84 | 0.58 | 0.09 |
| K ₂ O/Na ₂ O | 0.38 | 0.75 | 1 | 0.25 | 0.26 | 1.73 | 2.17 |
| Mg # | 68 | 69 | 69 | 47 | 53 | 59 | 48 |
| Rb | 28 | 41 | 54 | 19 | 31 | 63 | 118 |
| Sr | 1052 | 995 | 935 | 569 | 690 | 1150 | 1180 |
| Ba | 248 | 449 | 478 | 375 | 342 | 1385 | 1969 |
| V | 252 | 265 | 263 | 161 | 145 | 306 | 249 |
| Cr | 720 | 689 | 662 | 38 | 108 | 238 | 30 |
| Co | 39 | 42 | 28 | 24 | 23 | 48.35 | 47 |
| Ni | 295 | 286 | 307 | 12 | 24 | 85 | 19 |
| Zr | 144 | 141 | 137 | 104 | 113 | 191 | 219 |
| Y | 18 | 22 | 20 | 18 | 15 | 24 | 22 |
| Nb | 9 | 10 | 10 | 4 | 7 | 19 | 23 |
| Hf | 0.83 | 0.66 | — | — | — | 1.68 | 2.83 |
| Ta | 0.34 | 0.33 | — | — | — | 0.71 | 1.12 |
| Th | 7.67 | 7.39 | — | — | — | 6.02 | 11.8 |
| U | 1.69 | 1.6 | — | — | — | 1.52 | 3.46 |
| Sc | 30 | 35 | — | 27 | 23 | 32 | 15 |
| La | 31.75 | 32.29 | — | — | — | 48.92 | 62.34 |
| Ce | 51.41 | 54.86 | — | — | — | 98.18 | 120.94 |
| Nd | 23.84 | 27.1 | — | — | — | 43.55 | 46.9 |
| Sm | 4.24 | 5.21 | — | — | — | 7.07 | 7.32 |
| Eu | 1.56 | 1.82 | — | — | — | 2.07 | 2.12 |
| Gd | 5.6 | 7.12 | — | — | — | 7.3 | 8.33 |
| Er | 1.33 | 1.67 | — | — | — | 1.58 | 1.6 |
| Yb | 1.72 | 1.8 | — | — | — | 1.21 | 1.35 |
| ΣREE | 121.45 | 131.87 | — | — | — | 209.88 | 250.90 |
| Eu _N /Eu* | 0.98 | 0.92 | — | — | — | 0.89 | 0.83 |
| Ce _N /Ce* | 0.98 | 0.98 | — | — | — | 1.12 | 1.18 |
| (La/Yb) _N | 12.31 | 11.96 | — | — | — | 26.95 | 30.79 |
| (Ce/Yb) _N | 7.60 | 7.75 | — | — | — | 20.64 | 22.78 |
| (La/Sm) _N | 4.61 | 3.81 | — | — | — | 4.26 | 5.24 |
| (La/Ce) _N | 1.62 | 1.54 | — | — | — | 1.31 | 1.35 |
| La/Yb | 18.46 | 17.94 | — | — | — | 40.43 | 46.18 |
| Nb/Y | 0.5 | 0.45 | 0.5 | 0.22 | 0.47 | 0.79 | 1.05 |
| Zr/Y | 8 | 6.41 | 6.85 | 5.78 | 7.53 | 7.96 | 9.95 |
| Zr/Nb | 16 | 14.1 | 13.7 | 26 | 16.14 | 10.05 | 9.52 |
| Ti/Zr | 47.84 | 48 | 48.97 | 45.5 | 30.75 | 45.16 | 51.42 |
| Ti/V | 27.34 | 25.54 | 25.51 | 29.39 | 23.96 | 28.19 | 45.23 |
| Th/Yb | 4.46 | 4.11 | — | — | — | 4.98 | 8.74 |
| Ta/Yb | 0.2 | 0.18 | — | — | — | 0.59 | 0.83 |

Table 1. Continued...

| | Alkaline | | | | | |
|------------------------------------|----------|--------|-------|-------|--------|-------|
| | Kd-2 | Kd-11A | Kd-12 | Kd-14 | Kd-11B | Kd-6 |
| SiO ₂ | 53.5 | 53.48 | 55.94 | 55.66 | 58.42 | 57.34 |
| TiO ₂ | 1.09 | 1.09 | 1.18 | 0.91 | 0.82 | 0.72 |
| Al ₂ O ₃ | 18.32 | 18.71 | 18.29 | 16.12 | 17.62 | 18.35 |
| Fe ₂ O ₃ | 7.98 | 7.64 | 6.22 | 8.41 | 6.04 | 7.15 |
| MnO | 0.12 | 0.1 | 0.09 | 0.15 | 0.11 | 0.13 |
| MgO | 4.01 | 4.13 | 3.61 | 3.46 | 2.99 | 2.81 |
| CaO | 7.54 | 6.29 | 7.44 | 5.71 | 6.82 | 6.13 |
| Na ₂ O | 3.19 | 4.43 | 3.64 | 4.94 | 3.9 | 3.41 |
| K ₂ O | 3.69 | 3.62 | 3.23 | 3.83 | 2.95 | 3.36 |
| P ₂ O ₅ | 0.56 | 0.49 | 0.38 | 0.8 | 0.32 | 0.57 |
| FeOt/MgO | 1.77 | 1.64 | 1.53 | 2.16 | 1.8 | 2.26 |
| Na ₂ O/K ₂ O | 0.58 | 1.22 | 1.13 | 1.29 | 1.32 | 1.01 |
| K ₂ O/Na ₂ O | 1.73 | 0.83 | 0.89 | 0.78 | 0.76 | 0.99 |
| Mg # | 50 | 52 | 54 | 45 | 50 | 44 |
| Rb | 88 | 91 | 60 | 85 | 65 | 66 |
| Sr | 1656 | 1357 | 1339 | 1434 | 1342 | 1228 |
| Ba | 1302 | 1882 | 1509 | 1656 | 1509 | 1730 |
| V | 179 | 238 | 166 | 172 | 141 | 121 |
| Cr | 46 | 35 | 55 | 6 | 93 | 43 |
| Co | 31 | 27 | 25 | 20 | 24 | 11 |
| Ni | 28 | 23 | 23 | 6 | 23 | 9 |
| Zr | 340 | 234 | 224 | 304 | 241 | 267 |
| Y | 25 | 20 | 20 | 25 | 18 | 24 |
| Nb | 24 | 22 | 21 | 24 | 23 | 21 |
| Hf | 3.93 | — | — | — | — | — |
| Ta | 1.46 | — | — | — | — | — |
| Th | 10.47 | — | — | — | — | — |
| U | 4.78 | — | — | — | — | — |
| Sc | 18 | 14 | 17 | 11 | 13 | 12 |
| La | 71.26 | — | — | — | — | — |
| Ce | 141.99 | — | — | — | — | — |
| Nd | 54.78 | — | — | — | — | — |
| Sm | 8.15 | — | — | — | — | — |
| Eu | 2.19 | — | — | — | — | — |
| Gd | 7.59 | — | — | — | — | — |
| Er | 1.62 | — | — | — | — | — |
| Yb | 1.35 | — | — | — | — | — |
| ΣREE | 288.93 | — | — | — | — | — |
| Eu _N /Eu* | 0.86 | — | — | — | — | — |
| Ce _N /Ce* | 1.20 | — | — | — | — | — |
| (La/Yb) _N | 35.19 | — | — | — | — | — |
| (Ce/Yb) _N | 26.75 | — | — | — | — | — |
| (La/Sm) _N | 5.38 | — | — | — | — | — |
| (La/Ce) _N | 1.32 | — | — | — | — | — |
| La/Yb | 52.79 | — | — | — | — | — |
| Nb/Y | 0.96 | 1.1 | 1.05 | 0.96 | 1.28 | 0.88 |
| Zr/Y | 13.6 | 11.7 | 11.2 | 12.16 | 13.39 | 11.13 |
| Zr/Nb | 14.17 | 10.64 | 10.67 | 12.67 | 10.48 | 12.71 |
| Ti/Zr | 19.2 | 27.9 | 31.55 | 17.93 | 20.38 | 16.15 |
| Ti/V | 36.48 | 27.43 | 42.58 | 31.69 | 34.84 | 35.64 |
| Th/Yb | 7.76 | — | — | — | — | — |
| Ta/Yb | 1.08 | — | — | — | — | — |

FeOt = Total iron as FeO, Mg # = 100xMg / (Mg+Fe⁺²), SiO₂-P₂O₅ are in %, Rb-Yb are in ppm, REE ratios with _N are chondrite Normalized (after Nakamura, 1974), REE with * are interpolated values (see text for details).

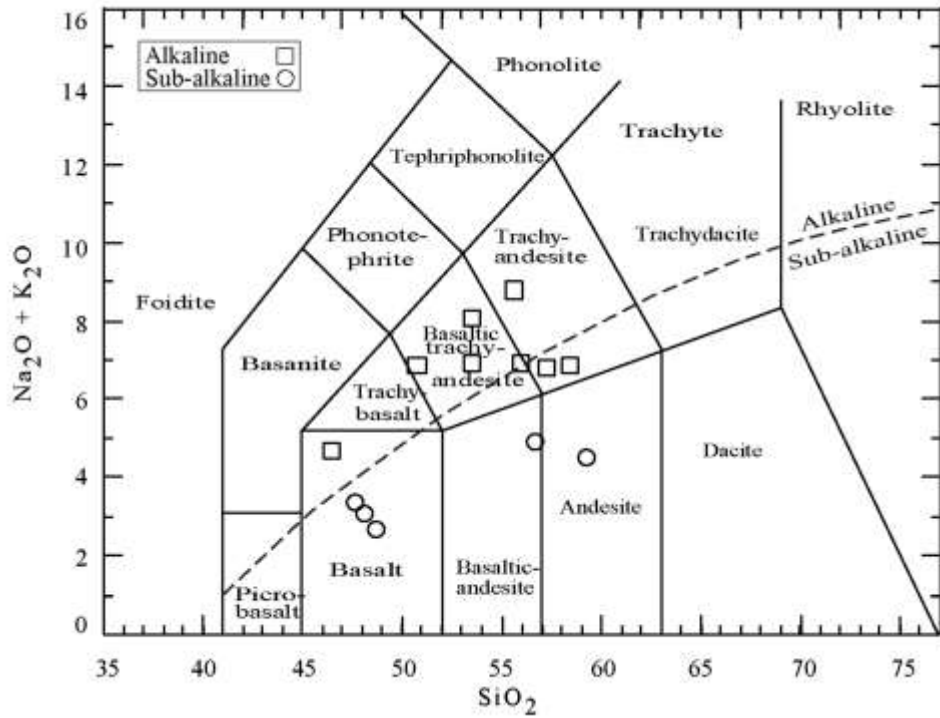


Fig. 5. Alkali versus SiO₂ classification scheme (after Le Bas, et al., 1986) for the Miocene volcanic rocks from the Chagai arc.

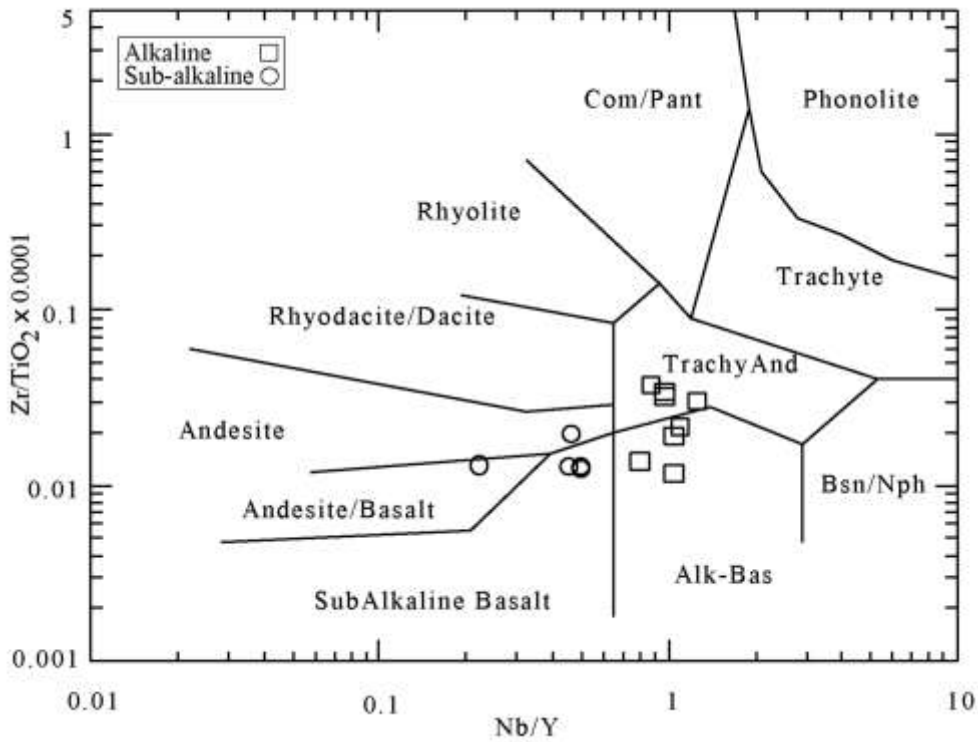


Fig. 6. Zr/Ti versus Nb/Y plot (after Winchester and Floyd, 1977) for the Late Cretaceous volcanic rocks from the Raskoh arc.

4.3 Major element geochemistry

4.3.1. Major element abundances

a) *Sub-alkaline Group*: The sub-alkaline Miocene volcanic rocks have wide ranges for SiO₂ (48.69-59.32 wt%) and TiO₂ (0.58-1.15 wt%) contents. These rocks also have widely varying amounts of Al₂O₃ (15.20-19.06 wt%) and Fe₂O₃ (6.35-10.44 wt%). Three of the basaltic sub-alkaline rocks have drastically high values for MgO contents (10.29-11.38 wt%) and are designated as high-magnesium (hereafter referred as h-mg) basalt, following Gill (1981) and Myers (1988). The other two andesitic rocks have normal MgO abundances (3.18-3.56 wt%), which are well below the reported (Gill, 1981; Myers, 1988) values of h-mg andesites (>6 wt% MgO). The CaO concentrations are also higher in h-mg basalts (10.29-11.39 wt%) as compared to andesites (7.11-7.96) in the same group. The h-mg basalts have low values and narrow range for Na₂O (1.66-1.90 wt%) and higher values and narrow range for K₂O (0.73-1.66 wt%) as compared to andesites in the same group (Table 1). The P₂O₅ concentrations are higher and exhibit limited variation (0.20-0.40 wt%). The h-mg basalts have low FeO/MgO ratios (0.81-0.84) and higher Mg # = $100 \times \text{Mg}/\text{Mg} + \text{Fe}^{2+}$ (68-69) as compared to andesites in the same group (Table 1).

b) *Alkaline Group*: The alkaline Miocene volcanic rocks also have wide overlapping ranges for SiO₂ (46.52-58.42 wt%) and higher abundances of TiO₂ (0.72-1.88 wt%) as compared to those of the sub-alkaline group (Table 1). This group also has higher abundance and narrow range for Al₂O₃ (16.12-19.12 wt%) and has higher overlapping range for Fe₂O₃ (6.04-11.43 wt%). One of the basalts from this group has high MgO (8.12 wt%), only a little lower than reported value (>9 wt% MgO) of high magnesium basalt by Gill (1981) and Myers (1988). The rocks in this group have lower (2.81-4.13 wt%) abundances of MgO. The CaO concentrations have lower range (5.71-9.84 wt%) in this group as compared to the sub-alkaline group. This group also has fairly higher abundances of Na₂O (1.70-4.94 wt%) and K₂O (2.94-4.69 wt%) as compared to the sub-alkaline group (Table 1). These characteristics are comparable with those of shoshonitic series of island arcs (Gill, 1981; Ewart, 1982). The P₂O₅ concentrations in this group are also higher (0.32-0.80 wt%) than the sub-alkaline group (Table 1). The rocks of this group have higher range of FeO/MgO ratios (1.25-2.26) and lower (44-59) overlapping Mg # ($100 \times \text{Mg}/\text{Mg} + \text{Fe}^{2+}$), which are consistent with the shoshonitic volcanic rocks of orogenic arcs (Gill, 1981).

4.3.2. Major element variations

The SiO₂ is used as fractionation index in various variation diagrams for major elements (Fig. 7). In these

diagrams all samples from the Miocene volcanic rocks show sharp to scattered negative correlation for MgO, CaO, Fe₂O₃, TiO₂, and P₂O₅ probably due to the fractionation of pyroxene, plagioclase, magnetite, ilmenite and sphene. Al₂O₃ generally exhibits negative correlation for alkaline rocks and positive for sub-alkaline rocks. Positive correlation of Al₂O₃ is due to its accumulation in the residual phase, while negative correlation is for fractionation of plagioclase. The Na₂O exhibits scattered positive correlation for the whole rock suite: probably due to enrichment of this element in the residual phase. The K₂O shows non-systematic scattered negative correlation with SiO₂ probably due to the partitioning of this element in the crystallizing phase of any K-bearing phase like orthoclase and hornblende, most probably the latter.

4.4. Trace element geochemistry

4.4.1. Trace element variations

In SiO₂ versus trace element variation diagrams (Fig. 8) Miocene volcanic rocks show non-systematic (scattered) positive trends for Ba, Sr and Zr, Ti, V, Sc, Ni and Co show scattered negative correlation. The negative trend for Ti, V and Sc is due to the fractionation of magnetite and ilmenite during magmatic differentiation. Similar scattered trends for Ni and Co are for the early fractionation of olivine and pyroxene.

4.4.2. Trace element abundances

Large ion lithophile elements (LILE): The Miocene volcanic rocks generally have higher abundances of LILE as compared to high field strength elements (HFSE). The LIL elements have considerably higher values in alkaline group rocks as compared to sub-alkaline group rocks. The Rb, Sr, Ba, Th and U in alkaline volcanic rocks range from 60 to 118 ppm, 1,150 to 1,656 ppm, 1,385 to 1,969 ppm, 6.02 to 11.80 ppm and 1.52 to 4.78 ppm respectively, which are consistent with shoshonitic volcanic rocks of orogenic arcs (Jacks and White, 1972; Ewart, 1982; Gill, 1981). The same elements in the sub-alkaline volcanic rocks range from 28 to 41 ppm, 569 to 1,052 ppm, 248 to 478 ppm, 7.39 to 7.67 ppm and 1.60 to 1.69 ppm respectively, which are consistent with medium to high-K calc-alkaline volcanic rocks of orogenic arcs (Jacks and White, 1972; Ewart, 1982; Gill, 1981).

High field strength elements (HFSE): The HFS elements have higher abundances in the alkaline group as compared to sub-alkaline group rocks. The Zr, Nb, Y, Hf and Ta in alkaline volcanic rocks range from 191 to 340 ppm, 19 to 24 ppm, 18 to 25 ppm, 1.68 to 2.83 ppm and 0.71 to 1.46 ppm respectively, which are again consistent with shoshonitic volcanic rocks of orogenic arcs (Jacks and White, 1972; Ewart, 1982; Gill, 1981).

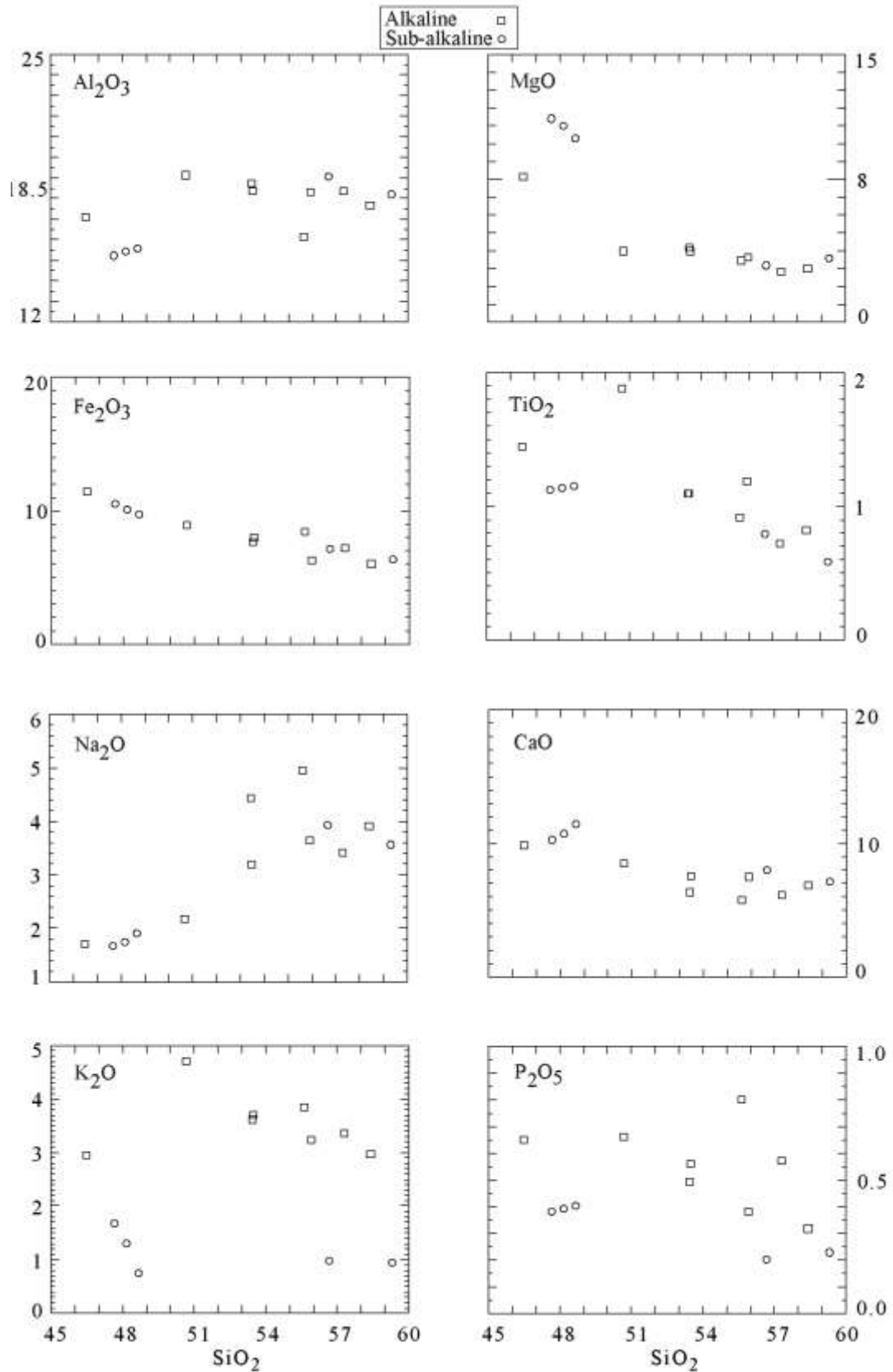


Fig. 7. Major element variation diagrams (with respect to SiO₂) showing fractionation trends in the Miocene volcanic rocks from the Chagai arc.

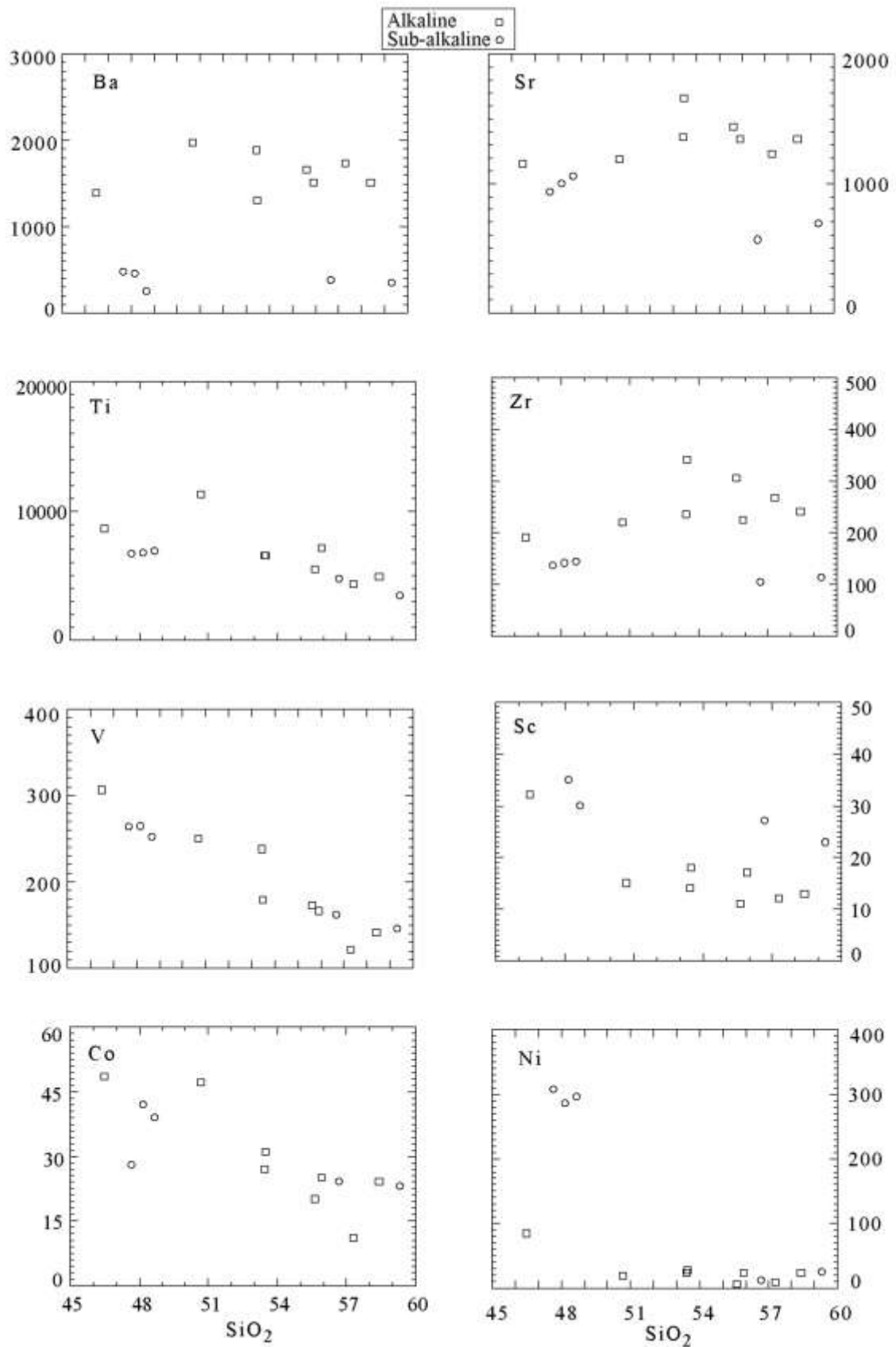


Fig. 8. Trace element variation diagrams (with respect to SiO_2) showing fractionation trends in the Miocene volcanic rocks from the Chagai arc.

The same elements in sub-alkaline volcanic rocks ranges from 113 to 144 ppm, 4 to 10 ppm, 15 to 22 ppm, 0.66 to 0.83 ppm and 0.33 to 0.34 ppm respectively, which are consistent with medium to high-K calc-alkaline volcanic rocks of orogenic arcs (Jacks and White, 1972; Ewart, 1982; Gill, 1981).

4.4.3. Spider diagrams

The multi-elements spider diagrams are generally used to study the behavior of incompatible trace elements in the rocks and to constrain their source regions, commonly with reference to primordial mantle or N-MORB compositions.

The incompatible trace element patterns (Fig. 9) of all the Miocene volcanic rocks exhibit considerable enrichment in all LIL incompatible elements relative to N-MORB. Amongst HFS incompatible elements Zr, Nb and P exhibit clear enrichment, while Ti and Y show variable enrichment and depletion relative to N-MORB, which is consistent with an enriched sub-arc mantle peridotite source. The spider patterns exhibit comparatively more enrichment of the whole range of incompatible trace elements in the alkaline volcanic rocks. These features in both the volcanic groups are again consistent with an enriched sub-arc mantle peridotite source. They also exhibit marked negative

slope from LILE to HFSE marking high LILE/HFSE ratios, which is suggestive of incorporation of higher amount of LILE enriched subduction related fluids in the sub-arc mantle magma source. In alkaline rocks this slope is steeper, thereby yielding much higher LILE/HFSE ratios and hence indicating excessive LILE enrichment of their parent magma by subduction related fluids. The patterns show negative Nb anomalies and positive spikes generally on Ba and Sr, which are consistent with island arc magmatism.

4.4.4. Compatible elements

The high magnesium sub-alkaline basaltic rocks have highest concentration of compatible elements: Cr = 662-720 ppm, Ni = 295-307 ppm, V = 252-265 ppm and Sc = 30-35 ppm. One of the basaltic rock samples from the alkaline volcanics also has high values for these elements and including Cr (238 ppm), Ni (85 ppm), Co (48.35 ppm), V (306 ppm) and Sc (32 ppm). This basalt also has the highest value for MgO (8.12 wt%) and Mg # (59), which suggests its derivation from a higher degree of partially melted and enriched mantle source as compared to the other alkaline rocks. Other volcanic rocks of alkaline and sub-alkaline groups have widely variable and lower abundances for these elements (Table 1).

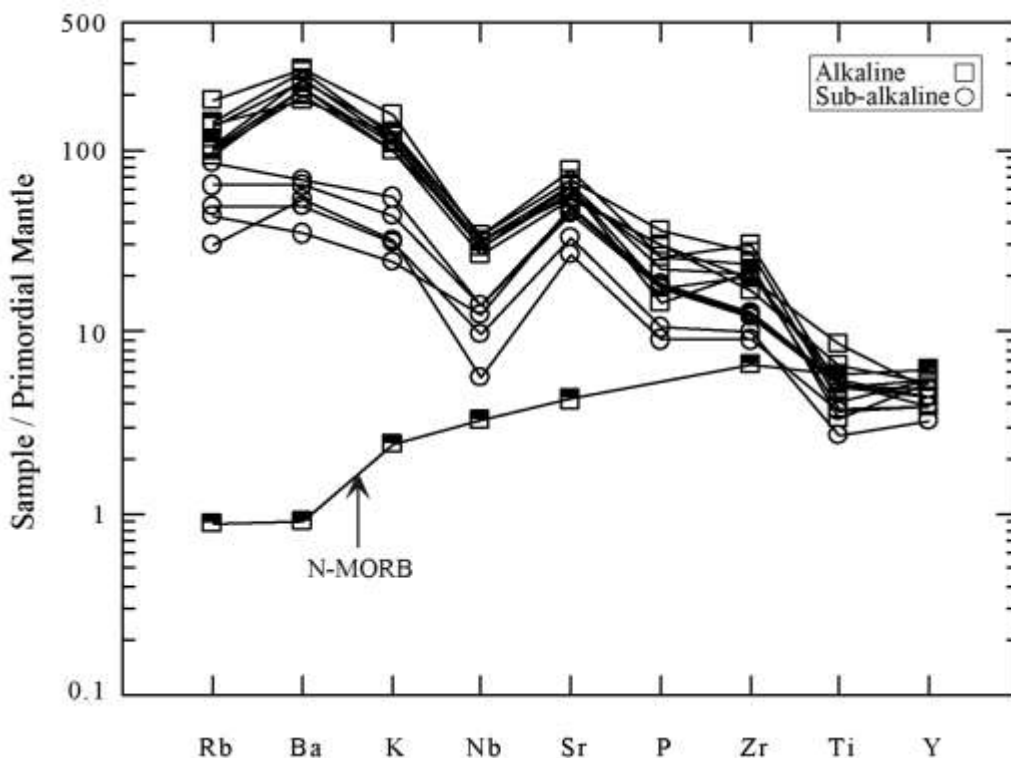


Fig. 9. Primordial mantle normalized spider diagram for the Miocene volcanic rocks from the Chagai arc. Average N-MORB and normalization values are after Sun and McDonough (1989).

4.5. Rare earth elements (REE)

The rare earth elements (La, Ce, Nd, Sm, Eu, Gd, Er and Yb) are analyzed in five samples (Kd-2, 5 and 9 from alkaline group and Kd-19 and 20 from sub-alkaline group). All the analyzed samples have higher concentrations of light rare earth elements (LREE) as compared to heavy rare earth elements (HREE). The alkaline volcanic rocks generally have considerably higher concentration of all the REE except Yb. The total REE (Σ REE) concentrations are also higher (209.88-288.93 ppm) in alkaline rocks relative to sub-alkaline rocks (121.45-131.87 ppm), which are consistent with shoshonitic and high-K calc-alkaline volcanic rocks of orogenic arcs respectively (Jacks and White, 1972; Ewart, 1982; Gill, 1981). The alkaline volcanic rocks also have higher normalized LREE/HREE ratios ($La_N/Yb_N = 26.95-35.19$ & $Ce_N/Yb_N = 20.64-26.75$) as compared to sub-alkaline volcanic rocks (Table 1). Both the volcanic group have a closer but narrow range of La_N/Ce_N (1.31-1.62) and La_N/Sm_N (3.81-5.38) ratios, which suggest a LREE enriched and less heterogeneous mantle source regions for the parent magma of these volcanic rocks. The measured Eu anomalies (Eu_N/Eu^*) are determined for Miocene rocks, which are calculated (after Taylor and McLennan, 1985) by dividing the chondrite normalized (Eu_N) values (after Nakamura, 1974) with the interpolated (Eu^*) values [$Eu_N/Eu^* = Eu_N/\sqrt{(Sm_N \times Gd_N)}$]. All the Miocene volcanic rocks have negative (< 1) Eu anomalies, which are consistent with plagioclase fractionation during differentiation. Similarly measured Ce anomalies (Ce_N/Ce^*) are also determined for these volcanics, which are calculated by dividing the chondrite normalized (after Nakamura, 1974) Ce values by the interpolated Ce values [$Ce_N/Ce^* = Ce_N/\sqrt{(La_N \times Nd_N)}$]. The alkaline rocks have positive Ce anomalies, whereas sub-alkaline volcanic rocks have negative Ce anomalies. The negative Ce anomalies indicate

involvement of fluids generated by the dehydration of pelagic sediments in the subducted slab (Gill, 1981) and are also noted in many other island arc volcanic rock suites including Japan arc (Masuda, 1968), Solomon island arc (Jacks and Gill, 1970) and Mariana arc (Hole et al., 1984). The positive Ce anomalies, negates the involvement of pelagic sediments from the subducted slab into their sub-arc mantle source (Gill, 1981).

4.5.1. Chondrite normalized REE diagrams

Chondrite normalized REE diagrams are generally prepared to determine the behavior of REE in the rocks and to constrain their source compositions, with reference to normalized chondritic values.

Chondrite normalized REE diagrams (Fig. 10) of Miocene volcanic rocks of the Chagai arc show enrichment of the whole range of REE except Er and Yb as compared to average N-MORB REE pattern (after Sun and McDonough, 1989). The sub-alkaline volcanic rocks show minor negative Ce anomalies, which suggest involvement of subducted pelagic sediments in the source (Hole et al., 1984). Most of the samples show variably developed negative Eu anomalies, which are generally linked with plagioclase fractionation during magmatic differentiation. The alkaline volcanic rocks exhibit comparatively more enrichment of whole range of REE, except Yb, relative to the sub-alkaline rocks. The chondrite normalized REE diagrams of Miocene volcanic rocks also exhibit marked negative slope from LREE to HREE giving high LREE/HREE ratios, which are suggestive of incorporation of higher amount of LREE enriched subduction related fluids in their sub-arc mantle magma source. In alkaline rocks this slope is steeper; because of enhanced LREE/HREE ratios due to excessive amount of LREE enriched subduction-related fluids in their magma source.

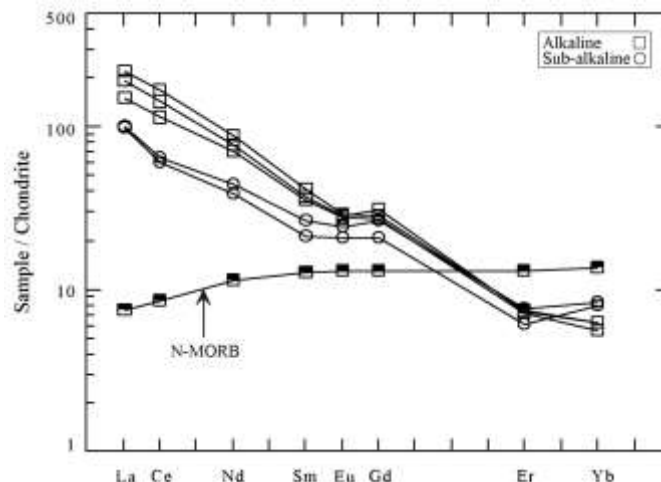


Fig. 10. Chondrite normalized REE diagram for the Miocene volcanic rocks from the Chagai arc. Average N-MORB values are after Sun and McDonough (1989), whereas normalization values are after Nakamura (1974).

5. Petrogenesis

5.1. Nature of source for parent magma

The criteria generally used to determine whether the basaltic rocks occurring in an area represent primary melts from the mantle peridotite source or these are the products of fractionated liquids, includes: (a) the presence of mantle peridotite (lherzolite) xenoliths within the basaltic volcanics series, (b) high magnesium number ($Mg \# = 100 \times Mg/Mg + Fe^{2+}$) and low FeO/MgO ratios, and (c) higher contents of compatible elements (Ni, Cr and Co).

The basaltic magma produced by up to 30% partial melting of mantle peridotite source must have Mg # in the range of 68-75 (Green, 1976; Frey et al., 1978; Hanson and Langmuir 1978). Gill (1981) has suggested a $Mg \# \geq 67$ and FeO/MgO ratios < 1.1 , whereas Tatsumi and Eggins (1995) have documented a $Mg \# > 70$ and FeO/MgO ratios < 1 for primary basaltic magmas. The basalts with 250-300 ppm Ni and 500-600 ppm Cr contents are considered to be derived from a primary mantle source (Perfit et al., 1980; Wilkinson and Le Maitre, 1987). The Co contents in primary basaltic magma must range from 27-80 ppm (Frey et al., 1978).

No mantle lherzolite xenolith is encountered from Miocene volcanic rock assemblage of the Chagai arc. The Mg # in the high-magnesium sub-alkaline Miocene basalts range from 68 to 69 and these rocks also have low (0.81-0.84) FeO/MgO. The same rocks also have higher contents of Ni (286-307 ppm), Cr (662-720 ppm) and Co (28-42 ppm). It is, therefore, suggested that the primary magma of the high magnesium sub-alkaline basalts have been directly derived from a sub-arc mantle peridotite source. Other sub-alkalic basaltic rocks have lower contents of magnesium, Ni, Co and Cr and have lower Mg # and higher FeO/MgO ratios, which do not fulfill the requirement of primary melts from the mantle peridotite source, hence parent magma of these rocks have been fractionated en route to eruption.

The alkaline volcanic rock series have higher Zr/Y, Ti/V, La/Yb and Ce/Yb and lower Zr/Nb and Ti/Zr ratios (than calc-alkaline rocks of island arcs), which are consistent with the ratios found in shoshonitic volcanic rocks of continental margin type arcs. Similarly values of these ratios in sub-alkaline volcanic rocks are more consistent with the calc-alkaline rocks of continental margin type arcs (Tables 1 and 2).

5.2. Tectonic setting

The SiO₂ versus FeO/MgO plot (Miyashiro, 1974) and classical FAM ternary diagram (Irvine and Baragar, 1971) are generally used to discriminate the tholeiitic and calc-alkaline series but provision to separate the

calc alkaline and shoshonite series is not available in these diagrams. The SiO₂ versus K₂O plot (Wilson, 1989) is generally used to separate low-K calc-alkaline, high-K calc-alkaline and shoshonite series. A plot of samples from the Miocene volcanic rocks in this diagram (Fig. 11A) reveals that all the sample except one from alkaline group plot in shoshonite series, whereas most of the sample from sub-alkaline series plot in calc-alkaline or high-K calc-alkaline series. For further confirmation of calc-alkaline and shoshonite parentage of Miocene volcanic rocks of Chagai arc the samples are again plotted (Fig. 11B) in Ta/Yb versus Ce/Yb diagram (after Pearce, 1982), which confirms the shoshonitic affinities of alkaline group. In Table 1 alkaline series Miocene rocks have higher contents of K₂O, Rb, Sr, Ba, Zr, Th, and U and have higher K₂O/Na₂O (~1), and lower K/Rb (~250), which are almost consistent with the reported (Jacks and White, 1972; Ewart, 1982) values of these elements in shoshonite series. To determine whether the Miocene volcanic rocks of the Chagai arc were erupted in an oceanic island arc environment or produced in a continental margin type arc settings, all the samples were plotted in Zr-Zr/Y plot (after Pearce, 1983). This plot (Fig. 11C) strongly supports that these rocks were erupted in a continental margin type arc setting. The discrimination diagrams based on trace element ratios are considered more authentic. A plot of various samples from the Miocene volcanic rocks in Th/Yb-Ta/Yb diagram (Pearce, 1983) further confirms their continental margin type island arc affinity and suggests that the parent magma of these volcanic rocks was generated by the partial melting of an enriched mantle source (Fig. 11D).

The spider patterns (Fig. 9), which exhibit positive spikes generally on K and Sr and with marked negative Nb anomalies further strongly confirm their island arc signatures (Pearce, 1982; Wilson, 1989; Saunders and Tarney, 1991). The marked negative Nb anomalies are explained by retention of this element in the residual phase during fractionation (Pearce, 1982; Wilson, 1989). The positive spikes or enrichment of certain LIL elements are generally considered to have formed by incorporation of these elements in the source from the subducting slab (Pearce, 1982; Wilson, 1989).

Nature of the source of parent magma: The Zr versus Zr/Y diagram (Fig. 11E) provides useful information about the nature of source, degree of partial melting and fractionation, etc. Plot of various rock samples from the Miocene volcanic rocks from the Chagai arc in this diagram (Pearce and Norry, 1979) indicates that these rocks are fractionated from about 15% partially melted enriched mantle source. Plot in Cr versus Y diagram (Fig. 11F), which is also designed (Pearce, 1982) for estimation of degree of partial melting and fractionation exhibits 15 to 25% partial melting of a mantle source.

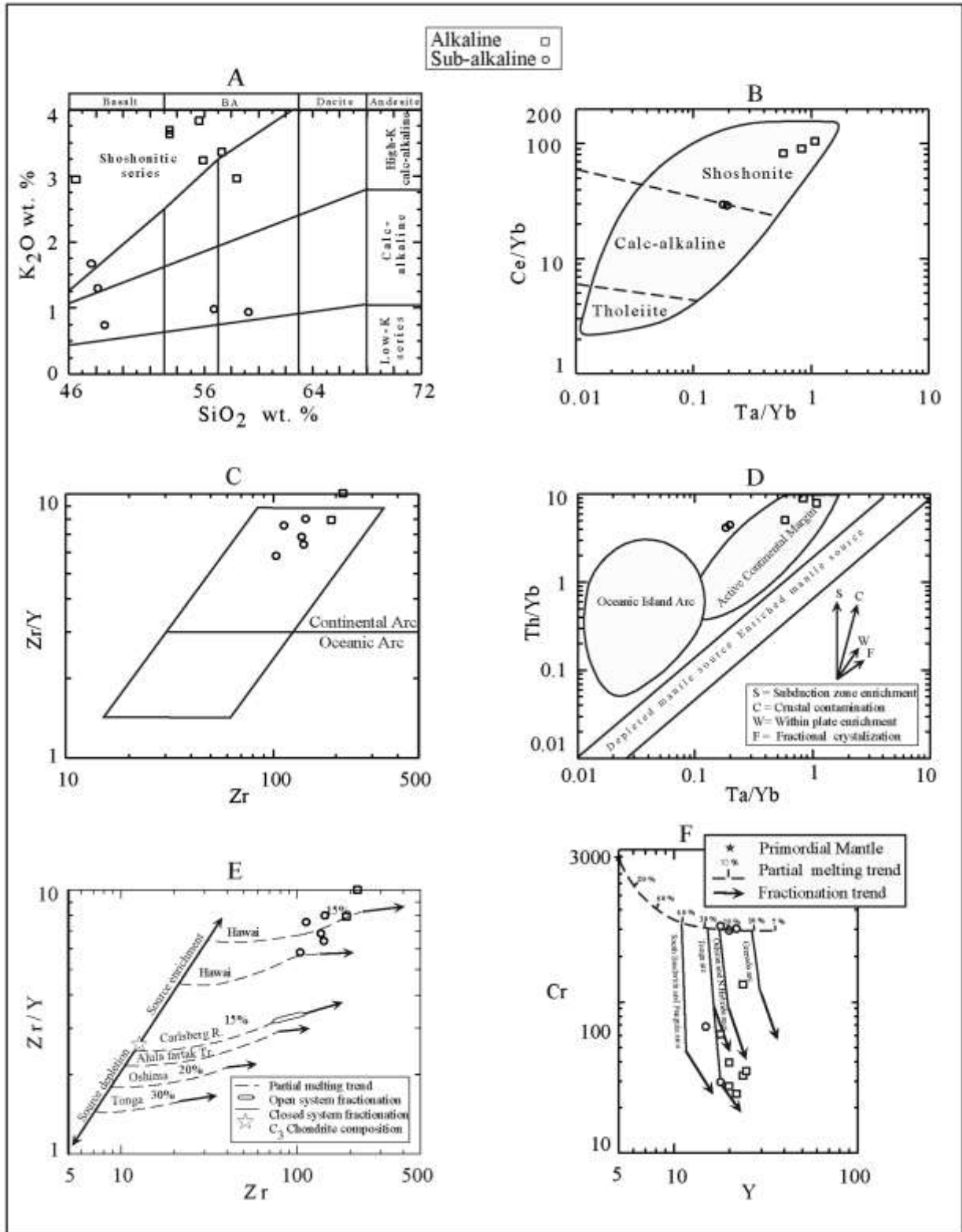


Fig. 11. Tectonomagmatic discrimination diagrams for the Miocene volcanic rocks from the Chagai arc.

In Table 2, average trace element chemistry of the Miocene calc-alkaline and shoshonitic volcanic rocks of the Chagai arc are compared with the average values of oceanic island arcs and continental margin type (Andes arc) arcs. This comparison shows close affinities of Miocene volcanic rocks of the Chagai arc with continental margin type arcs rather than oceanic island arcs.

6. Porphyry Copper Mineralization

A total numbers of 48 porphyry copper occurrences have been reported in the Chagai arc, which are generally hosted in Oligocene-Miocene granitoids stocks (Sillitoe, 1978; Siddiqui and Khan, 1986; Siddiqui 1996; Perello et al., 2008). Out of these settings, five are more important, because of their higher tonnage and extent of investigation (Fig. 1). They include the well known Saindak and Reko Diq porphyry deposits and lesser known porphyry copper prospects of Missi, Ziarat Pir Sultan and Dasht-e-Kain. These deposits collectively have about 10000 million tons of Cu (0.35–0.70%) with trace amount of Mo (0.01–0.015%) and Au (0.1– 6.50 g/t).

Hydrothermal alterations in these porphyry copper occurrences are mainly associated with tonalite porphyry stocks, except Missi prospect, which occurs in a marginal part of a granodiorite batholith. Hydrothermal alteration is generally developed in a concentric zonal pattern as reported for western American deposits by Lowell and Guilbert (1970). Potassium silicate alteration zone (K-zone) generally occurs usually within the intrusive porphyry stock, but in Saindak and Koh Dalil-Reko Diq deposits some of the adjacent wall rock sediments have also been affected by the K-alteration. Argillic alteration only occur as small isolated patches within the phyllic zone rather than a regular argillic alteration zone in all the porphyry copper setting. Phyllic (quartz sericitic) alteration zones are developed in all the occurrences as continuous or semi-continuous haloes around the K-zone. Propylitic alteration zone are also developed in all of the occurrences and encircles the phyllic alteration zone.

A comparison of the primordial mantle normalized incompatible trace elements and chondrite normalized REE patterns of the Eocene, Oligocene, Miocene and Plio-Pleistocene volcanics show relatively more enrichment of LILE and LREE in the Oligocene and Miocene volcanics (Fig. 12). This suggests that during the Oligocene-Miocene period which is the time of emplacement of several porphyry copper deposits in the Chagai arc; comparatively more LILE and LREE enriched fluids from the subducting slab of oceanic crust were added to the sub-arc mantle source regions of these volcanics.

The Oligocene-Miocene magmatism in the Chagai arc is not only represented by volcanic and volcanoclastic but is also represented by several large batholiths and small barren and porphyry copper hosting stocks which appears to be the cupolas of larger subsurface batholiths (Fig. 1). The Oligocene and Miocene volcanics show continental margin type calc-alkaline affinities and are produced from a highly enriched mantle source (Siddiqui, 2004). Such highly enriched calc-alkaline volcanics are generally produced in island arcs with shallow subduction zones (Wilson, 1989), which are generally controlled by the convergence rate, density and age of subducting plate (Cross and Pilger, 1982; Jarrard, 1986). A higher convergence rate and convergence of a relatively younger and low-density crust result in shallow subduction (Wilson, 1989). It is suggested that relatively higher rate of convergence was developed during Oligocene-Miocene period due to the opening of the Red Sea (Girdler, 1978) and relatively rapid spreading in the Carlsberg Ridge. Moreover, the oceanic crust, which subducted during this period, was relatively younger and hence less dense than the older crust (Cross and Pilger, 1982; Wilson, 1989). It is, therefore, suggested that during the Oligocene-Miocene period, relatively higher quantities of subduction related fluids (enriched in LILE and LREE) were added to the sub-arc mantle source.

7. Conclusions

The petrogenetic studies suggest that Miocene volcanic rocks of the Chagai arc represent a calc-alkaline and shoshonite series. The studies further suggest that these rocks were erupted in a continental margin type arc rather than an oceanic island arc setting. Enrichment of most incompatible trace elements, Σ REE and greatly enhanced Zr/Y, Ti/V, Ta/Yb, Th/Yb, La/Yb and Th/Yb ratios relative to N-MORB indicate that parent magma of both the volcanic groups was derived from an enriched sub-arc mantle source. The calc-alkaline basaltic rocks have high magnesium MgO (8.12-11.38 wt%) Mg # (68-69), Co (28-42 ppm), Ni (286-307 ppm) and Cr (662-720 ppm). These features suggest that parent magma of these rocks has been directly derived from the partial melting of a sub-arc mantle source. The higher values of K, Rb, Sr, Ba, Zr, Th, and U and enhanced LILE/HFSE and LREE/REE ratios suggests incorporation of greater amount of subduction related fluid into the sub-arc mantle source. The Z-Z/Y and Cr-Y studies suggests that parent magma of these rock suites was generated by about 15-25% partial melting of an enriched sub-arc mantle source and fractionated in an upper level magma chamber. A comparison of the primordial mantle normalized incompatible trace elements and chondrite normalized REE patterns of Eocene, Oligocene,

Table 2. A comparison of average trace element chemistry of Miocene volcanic rocks of the Chagai arc with some arc related volcanic rocks of the world.

| Element | Average Miocene volcanic rocks from the Chagai Arc | | | | | | Andes Arc (a) | | | Western USA Arc (b) | | | South West Pacific Arc (c) |
|---------|--|--------|----------------------|----------|---------------|----------|------------------|----------------------|----------|------------------------|----------------------|----------|----------------------------------|
| | Shoshonite | | | | Calc alkaline | | Calc alkaline | | | Shoshonite | | | Shoshonitic Basalt |
| | Basalt (h-Mg) | Basalt | Basaltic Andesite | Andesite | Basalt | Andesite | Basalt | Basaltic Andesite | Andesite | Basalt | Basaltic andesite | Andesite | |
| K | 24402 | 38927 | 29818 | 26187 | 10181 | 7885 | 11786 | 13446 | 22161 | 18011 | 31125 | 35275 | 23240 |
| Ti | 8626 | 11261 | 6394 | 4612 | 6789 | 4103 | 6829 | 7607 | 5691 | 12280 | 6709 | 6050 | 5451 |
| Rb | 63 | 118 | 81 | 65.5 | 41 | 25 | 50 | 45 | 75 | 47.4 | 130 | 139 | 68.8 |
| Sr | 1150 | 1180 | 1446.5 | 1285 | 994 | 629.5 | 608 | 644 | 648 | 1057 | 1043 | 902 | 995 |
| Ba | 1385 | 1969 | 1588 | 1620 | 392 | 358.5 | 345 | 676 | 886 | 1149 | 1593 | 2017 | 599 |
| V | 306 | 249 | 188.75 | 131 | 260 | 153 | 187 | 220 | 125 | 199 | 210 | 80.2 | 261 |
| Cr | 238 | 30 | 35.5 | 68 | 690.33 | 73 | 68 | 202 | 48 | 82.5 | 196 | 65.9 | 189 |
| Co | 48.35 | 47 | 25.75 | 17.5 | 36.33 | 23.5 | 30 | 31 | 19 | 56.3 | 28 | 15.4 | 32.8 |
| Ni | 85 | 19 | 20 | 16 | 296 | 18 | 58 | 67 | 39 | 80.3 | 63.3 | 59.2 | 76.2 |
| Zr | 191 | 219 | 275.5 | 254 | 140.67 | 108.5 | 162 | 179 | 195 | 225 | 226 | 394 | 82.5 |
| Y | 24 | 22 | 22.5 | 21 | 20 | 16.5 | 30 | 25 | 12 | 35.5 | 26.3 | 26 | 18.7 |
| Nb | 19 | 23 | 22.75 | 22 | 9.67 | 5.5 | — | 13 | — | 32.5 | 15 | 16.3 | 5.7 |
| Hf | 1.68 | 2.83 | 3.93 | 0.75 | — | — | 2.9 | 3.67 | 5.46 | — | — | — | 1.0 |
| Ta | 0.71 | 1.12 | 1.46 | 0.34 | — | — | — | — | — | — | — | — | — |
| Th | 6.02 | 11.8 | 10.47 | 7.53 | — | — | — | — | — | — | — | — | — |
| U | 1.52 | 3.46 | 4.78 | 1.65 | — | — | — | — | — | — | — | — | — |
| Sc | 32 | 15 | 15 | 12.5 | 32.5 | 25 | — | — | — | — | — | — | — |
| Cu | — | — | — | — | — | — | 30 | 49.6 | 40 | 44.5 | 152 | 27.2 | 130 |
| La | 48.92 | 62.34 | 71.26 | — | 32.02 | — | 16.3 | 24.6 | 38 | 115 | 70 | 150 | 18.8 |
| Ce | 98.18 | 120.94 | 141.99 | — | 53.14 | — | 41.6 | 51.3 | 66.8 | 200 | 80 | 200 | 35.4 |
| Nd | 43.55 | 46.9 | 54.78 | — | 25.47 | — | — | — | — | — | — | — | — |
| Sm | 7.07 | 7.32 | 8.15 | — | 4.73 | — | — | — | — | — | — | — | — |
| Eu | 2.07 | 2.12 | 2.19 | — | 1.69 | — | — | — | — | — | — | — | — |
| Gd | 7.3 | 8.33 | 7.59 | — | 6.36 | — | — | — | — | — | — | — | — |
| Er | 1.58 | 1.6 | 1.62 | — | 1.5 | — | — | — | — | — | — | — | — |
| Yb | 1.21 | 1.35 | 1.35 | — | 1.76 | — | 2.29 | 2.32 | 1.94 | 3.0 | 3.0 | 2.4 | 1.6 |
| Ti/V | 28.19 | 45.23 | 34.54 | 35.24 | 26.13 | 26.68 | 36.58 | 34.64 | 45.60 | 61.71 | 31.95 | 75.44 | 20.89 |
| Zr/Y | 7.96 | 9.95 | 12.17 | 12.26 | 7.09 | 6.66 | 5.23 | 7.04 | 15.98 | 6.34 | 8.59 | 15.15 | 4.41 |
| Ti/Zr | 45.16 | 51.42 | 24.15 | 18.27 | 48.27 | 38.12 | 42.22 | 42.57 | 29.23 | 54.58 | 29.69 | 15.35 | 66.07 |
| Zr/Nb | 10.05 | 9.52 | 12.03 | 11.6 | 14.6 | 21.07 | — | 14.32 | — | 6.92 | 15.07 | 24.17 | 14.47 |
| Y/Nb | 1.26 | 0.96 | 0.99 | 0.96 | 2.07 | 3.32 | — | — | — | 1.09 | 1.75 | 1.60 | 3.28 |
| K/Rb | 387 | 368.12 | 356.13 | 399.62 | 244.23 | 336.37 | — | — | 273 | 379.98 | 239.42 | 253.78 | 337.79 |
| La/Yb | 40.43 | 46.18 | 52.79 | — | 18.2 | — | 7.12 | 10.60 | 19.49 | 38.33 | 23.33 | 62.5 | 11.75 |
| Ce/Yb | 81.14 | 89.59 | 105.18 | — | 30.18 | — | 2.55 | 22.11 | 34.43 | 66.67 | 26.67 | 83.33 | 22.13 |

The values in columns (a), (b) and (c) are after Ewart (1982). All the data is in ppm.

Miocene and Plio-Pleistocene volcanics show relatively more enrichment of LILE and LREE in the Oligocene and Miocene volcanics. This suggests that during that period, which is also the time of emplacement of several porphyry copper deposits in the Chagai arc;

relatively higher quantities of subduction related fluids enriched in LILE and LREE were added to the sub-arc mantle source from the subducting slab of the oceanic crust.

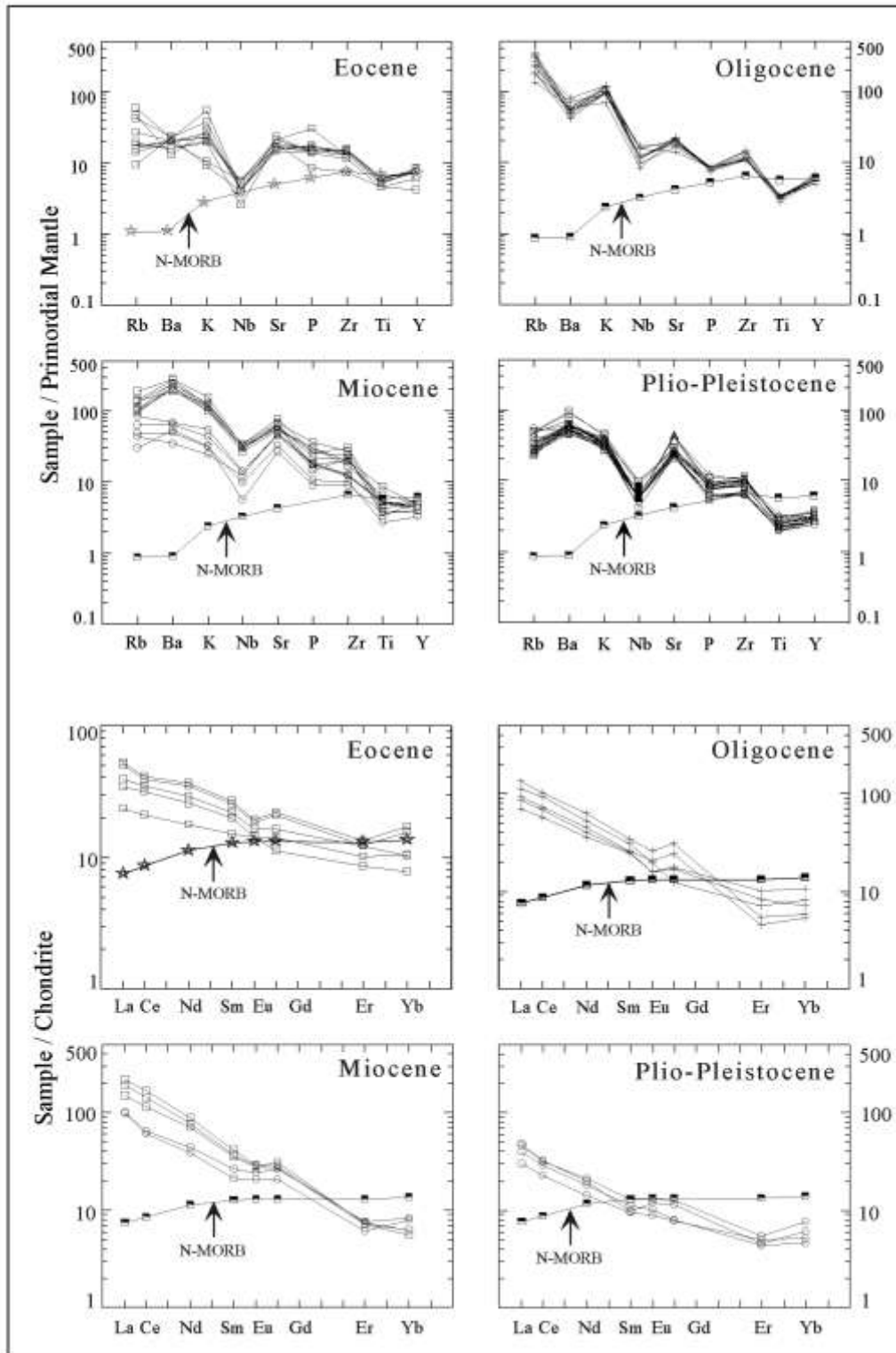


Fig. 12. Comparison of Primordial mantle normalized (after Sun and McDonough, 1989) spider and Chondrite normalized (after Nakamura, 1974) REE diagrams for the Eocene-Pleistocene volcanic rocks from the Chagai arc. Average N-MORB values are after Sun and McDonough (1989).

Acknowledgements

The authors are indebted to Mr. S. Hasan Gauhar, ex-Director General, Geological Survey of Pakistan (GSP) and Mr. Muhammad Sakhawat, Ex-Director, Geoscience Lab for the arrangement of funds for field and laboratory research, their moral support and encouragement at every step during research. Dr. M. Mikoshiba is greatly acknowledged for the guidance and help during REE analysis in the Geochemical Laboratory of the Geological Survey of Japan. The authors are also gratefully thankful to Professors N.U. Khattak and M. Arif for critical review and constructive suggestions.

References

- Ahmed, M. U., 1984. Geological exploration and preliminary evaluation of Dasht-e-Kain porphyry copper-molybdenum prospect Chagai district, Balochistan, Pakistan. Unpublished Ph.D. Thesis, University of Belgrade, Yugoslavia.
- Arthurton, R. S., Alam, G. S., Ahmed, S. A., Iqbal, S., 1979. Geological history of Alam Reg -Mashki Chah area, Chagai District, Balochistan. In: Farah, A., DeJong, K. A. (Eds.), *Geodynamics of Pakistan*. Geological Survey of Pakistan, 325-331.
- Bakr, M. A., Jackson, R. O., 1964. Geological Map of Pakistan. Geological Survey of Pakistan, Quetta.
- Britzman, L., 1979. Fission track ages of intrusives of Chagai District, Balochistan, Pakistan. Unpublished M.A. Thesis, Dartmouth College, Hanover, N. H., U.S.A.
- Cross, T. A., Pilger, R. H., 1982. Control on subduction geometry, location of magmatic arcs and tectonics of arcs and back arc basins. *Geological Society of America Bulletin*, 93, 545-562.
- Dykstra, J. D., 1978. A geological study of Chagai Hills Balochistan, Pakistan using LANDSAT digital data. Unpublished Ph.D. Thesis, Dartmouth College, Hanover, N. H., U.S.A.
- Ewart, A., 1982. The mineralogy and petrology of Tertiary-Recent orogenic volcanic rocks with special reference to andesitic-basaltic compositional range, In: Throp, R. S., (Ed.), *Andesites: Orogenic Andesites and Related Rocks*. John Wiley and Sons, New York, 26-87.
- Farah, A., Abbas G., DeJong, K. A., Lawrence, R. D., 1984. Evolution of the Lithosphere in Pakistan. *Tectonophysics*, 105, 207-227.
- Frey, F. A., Green, D. H., Roy, S. D., 1978. Integrated model for basalt petrogenesis: A study of quartz tholeiites to olivine melilite from southeastern Australia, utilizing geochemical and experimental petrological data. *Journal of Petrology*, 19, 463-513.
- Fyfe, W. S., 1976. Hydrosphere and continental crust. *Geoscience Canada*, 3, 255-268.
- Gill, J. B., 1981. *Orogenic Andesites and Plate Tectonics*. Springer, Berlin.
- Govindaraju, K., 1989. Working Group on Analytical standards of minerals, ores and rocks. *Geostandards Newsletter (Special Issue)*, France, 13, 114.
- Green, D. H., 1976. Experimental studies on a modal upper mantle composition at high pressure under water saturated and water undersaturated conditions: *Canadian Mineralogist*, 14, 255-268.
- Hanson, G. N., Langmuir, C. H., 1978. Modeling of major elements in mantle-melts systems using trace element approaches. *Geochimica et Cosmochimica Acta*, 42, 725-742.
- Girdler, R. W., 1978. Comparison of East African rift system and the Permian Oslo, In: Neuman, E. R., Ramberg, I. B. (Eds.), *Tectonics and Geophysics of Continental Rifts*. D. Riedel Dor Drecht, 329-345.
- Hole, M. J., Saunder, A. D., Marriner, G. F., Tarney, J., 1984. Subduction of pelagic sediments; implication for the origin of Ce-anomalous basalts from Mariana Islands. *Journal of Geological Society London*, 141, 453-472.
- Hunting Survey Corporation Limited, 1960. *Reconnaissance Geology of Part of West Pakistan*. A Colombo Plan Cooperative Project, Government of Canada, Toronto, Canada, 550.
- Imai, N., 1990. Multielement analysis of rock with the use of geological certified reference materials by inductively coupled plasma mass spectrometry. *Analytical Science*, 6, 389-385.
- Irvine, T. N., Baragar, W. R. A., 1971. A guide to the chemical classification of the common volcanic rocks. *Canadian Journal of Earth Sciences*, 8, 523-548.
- Jacks, P., Gill, J. B., 1970. Rare earth elements and the island arc tholeiitic series. *Earth and Planetary Science Letters*, 9, 17-28.
- Jacks, P., White, J. R., 1972. Major and trace element abundances in volcanic rocks of orogenic areas. *Geological Society of America Bulletin*, 83, 29-40.
- Jarrard, R. D., 1986. Relation among subduction parameters. *Reviews of Geophysics*, 24, 217-284.
- Jones, A. G., 1960. *Reconnaissance Geology of Part of West Pakistan*. A Colombo Plan Cooperative Project, Government of Canada, Toronto, (Hunting Survey Corporation report), 550.

- Khan, F., Ahmed, W., 1981. Geological map of Koh-e-Dalil Quadrangle, Chagai District, Balochistan, Pakistan. Geological Survey of Pakistan, Quetta.
- Le Bas, M. J., Le Maitre, R. W., Streckeisen, A., Zanettin, B., 1986. A chemical classification of volcanic rocks based on the total alkali silica diagram. *Journal of Petrology*, 27, 745-750.
- Lowell, J. D., Guilbert, J. M., 1970. Lateral and vertical alteration mineralization zoning in porphyry ore deposits. *Economic Geology*, 65, 373-408.
- Masuda, A., 1968. Geochemistry of Lanthanides in basalts of central Japan. *Earth and Planetary Science Letters*, 4, 284-292.
- Miyashiro, A., 1974. Volcanic rock series in island arcs and active continental margins. *American Journal of Science*, 274, 321-355.
- Myers, J. D., 1988. Possible petrogenetic relations between low and high MgO Aleutian basalts. *Geological Society of America Bulletin*, 100, 1040-1053.
- Nakamura, N., 1974. Determination of REE, Ba, Fe, Mg, Na and K in carbonaceous and ordinary chondrites. *Geochimica et Cosmochimica Acta*, 38, 757-775.
- Nigell, R. H., 1975. Reconnaissance of the geology and ore mineralization in part of the Chagai District, Balochistan, Pakistan. U. S. Geological Survey, Project Report, PK-27, 550.
- Ogg, J. G., Ogg, G., Gradstein, F. M., 2008. The Concise Geological Time Scale, International Commission on Stratigraphy (www.stratigraphy.org).
- Pearce, J. A., Norry, M., 1979. Petrogenetic implications of Ti, Zr, Y and Nb variation in volcanic rocks. *Contributions to Mineralogy and Petrology*, 69, 33-47.
- Pearce, J. A., 1982. Trace elements characteristics of lavas from destructive plate boundaries. In: Throp, R. S., (Ed.), *Andesites: Orogenic Andesites and Related rocks*. John Wiley and Sons, New York, 525-548.
- Pearce, J. A., 1983. The role of subcontinental lithosphere in the magma genesis at destructive plate margin. In: Hawkes-worth, C. J., Norry, M. J., (Eds.), *Continental Basalts and Mantle Xenoliths*. Natwich Shiva, 230-249.
- Perfit, M. R., Gust, D. A., Bence, A. E., Arculus, R. J., Taylor, S. R., 1980. Chemical characteristics of island arc basalts: implications for mantle sources. *Chemical Geology*, 30, 227-256.
- Perello, J., Raziq, A., Schloderer, J., Rehman, A. U., 2008. The Chagai Porphyry Copper Belt, Baluchistan Province, Pakistan. *Economic Geology*, 103, 1583-1612.
- Saunders, A. D., Tarney, J., 1991. Back-arc basins. In: Floyd, P.A. (Ed.), *Oceanic Basalts*. Blackie, London, 219-263.
- Siddiqui, R. H., Khan, W., Haque, M., 1986. Petrological and petrochemical studies of northcentral Chagai Belt and its tectonic implications. *Acta Mineralogica Pakistanica*, 2, 12-23.
- Siddiqui, R. H., Khan, W., 1986. A comparison of hydrothermal alteration in porphyry copper mineralization of Chagai calc-alkaline magmatic Belt Balochistan, Pakistan. *Acta Mineralogica Pakistanica*, 2, 100-106.
- Siddiqui, R. H., Hussain, S. A., Haque, M., 1987. Geology and petrography of Eocene mafic lavas of Chagai island arc, Balochistan, Pakistan. *Acta Mineralogica Pakistanica*, 3, 123-128.
- Siddiqui, R. H., Haque, M., Hussain, S. A., 1988. Geology and petrography of Paleocene mafic lavas of Chagai island arc, Balochistan, Pakistan. Geological Survey of Pakistan, Information Release, 361, 18.
- Siddiqui, R. H., 1996. Magmatic evolution of Chagai-Raskoh arc terrane and its implication for porphyry copper mineralization. *Geologica*, 2, 87-119.
- Siddiqui, R. H., 2004. Crustal evolution of the Chagai-Raskoh arc terrane, Balochistan, Pakistan. Unpublished Ph.D. Thesis, University of Peshawar, Pakistan.
- Sillitoe, R. H., 1978. Metallogenic evolution of a collision mountain belt in Pakistan: a preliminary analysis. *Journal of Geological Society of London*, 125, 377-387.
- Spector, A. and Associates Ltd., 1981. Report on interpretation of aeromagnetic survey data, Balochistan Province, Pakistan. Project Report, J-223, 107.
- Sun, S. S., McDonough, W. F., 1989. Chemical and isotopic systematics of ocean basalt, implication for mantle composition and processes. In: Saunders, A. D., Torny, M. J. (Eds.), *Magmatism in the Ocean Basins*. Geological Society of London Special publication, 42, 313-345.
- Tatsumi, Y., Eggins, S., 1995. Subduction zone magmatism. Blackwell Science, Oxford, England.
- Taylor, S. R., McLennan, S. M., 1985. The continental crust: its composition and evolution. Blackwell, Oxford.
- Vredenburg, E. W., 1901. A geological sketch of the Balochistan desert and part of Eastern Persia. Geological Survey of India, Memoir 302.
- Wilkinson, J. F. G., Le Maitre, R. W., 1987. Upper mantle amphiboles and micas and TiO₂, K₂O and P₂O₅ abundances and 100 × Mg / (Mg+Fe⁺²) ratios of common basalts and undepleted mantle compositions. *Journal of Petrology*, 28, 37-73.
- Wilson, M., 1989. *Igneous Petrogenesis*. Unwin and Hyman, London.
- Winchester, J. A., Floyd, P. A., 1977. Geochemical discrimination of different magma series and their differentiation products using immobile elements. *Chemical Geology*, 20, 325-343.